Available online at www.sciencedirect.com
SCIENCE DIRECT®
Catalysis Today 98 (2004) 463–484
CATALYSIS TODAY
www.elsevier.com/locate/cattod

Tri-reforming of methane: a novel concept for catalytic production of industrially useful synthesis gas with desired H_2/CO ratios☆

Chunshan Song*, Wei Pan

Clean Fuels and Catalysis Program, The Energy Institute, and Department of Energy and Geo-Environmental Engineering, Pennsylvania State University, 209 Academic Projects Building, University Park, PA 16802, USA

Abstract

A novel process concept called tri-reforming of methane has been proposed in our laboratory using CO_2 in the flue gases from fossil fuel-based power plants without CO_2 separation [C. Song, Chemical Innovation 31 (2001) 21–26]. The proposed tri-reforming process is a synergetic combination of CO_2 reforming, steam reforming, and partial oxidation of methane in a single reactor for effective production of industrially useful synthesis gas (syngas). Both experimental testing and computational analysis show that tri-reforming can not only produce synthesis gas (CO + H_2) with desired H_2/CO ratios (1.5–2.0), but also could eliminate carbon formation which is usually a serious problem in the CO_2 reforming of methane. These two advantages have been demonstrated by tri-reforming of CH_4 in a fixed-bed flow reactor at 850 °C with supported nickel catalysts. Over 95% CH_4 conversion and about 80% CO_2 conversion can be achieved in tri-reforming over Ni catalysts supported on an oxide substrate. The type and nature of catalysts have a significant impact on CO_2 conversion in the presence of H_2O and O_2 in tri-reforming in the temperature range of 700–850 °C. Among all the catalysts tested for tri-reforming, their ability to enhance the conversion of CO_2 follows the order of Ni/MgO > Ni/MgO/CeZrO > $Ni/CeO_2 \approx Ni/ZrO_2 \approx Ni/Al_2O_3$ > Ni/CeZrO. The higher CO_2 conversion over Ni/MgO and Ni/MgO/CeZrO in tri-reforming may be related to the interaction of CO_2 with MgO and more interface between Ni and MgO resulting from the formation of NiO/MgO solid solution. Results of catalytic performance tests over Ni/MgO/CeZrO catalysts at 850 °C and 1 atm with different feed compositions confirm the predicted equilibrium conversions based on the thermodynamic analysis for tri-reforming of methane. Kinetics of tri-reforming were also examined. The reaction orders with respect to partial pressures of CO_2 and H_2O are different over Ni/MgO, Ni/MgO/CeZrO, and Ni/Al_2O_3 catalysts for tri-reforming.

Keywords: Tri-reforming; CO_2 reforming; Steam reforming; Synthesis gas; Catalyst

1. Introduction

CO_2 conversion and utilization are an important element in chemical research on sustainable development, because CO_2 also represents an important source of carbon for fuels and chemical feedstock in the future [1–3]. The prevailing thinking for CO_2 conversion and utilization begins with the use of pure CO_2, which can be obtained by separation. In general, CO_2 can be separated, recovered and purified from concentrated CO_2 sources by two or more steps based on either absorption or adsorption or membrane separation. Even the recovery of CO_2 from concentrated sources requires substantial energy input [4,5]. According to US DOE, current CO_2 separation processes alone require significant amount of energy which reduces a power plant's net electricity output by as much as 20% [4,6].

This paper discusses a new process concept that has been recently proposed in our laboratory [7–9] for effective production of synthesis gas (CO + H_2) with desired H_2/CO ratios using CO_2 in the flue gases from electric power plants without CO_2 pre-separation. The proposed tri-reforming process is a synergetic combination of CO_2 reforming, steam

☆ Based on an invited keynote lecture by C. Song at the 227th American Chemical Society National Meeting during March 28–April 1, 2004 in Anaheim, CA.

* Corresponding author. Tel.: +1 814 863 4466; fax: +1 814 865 3248.
E-mail address: csong@psu.edu (C. Song).

0920-5861/$ – see front matter © 2004 Elsevier B.V. All rights reserved.
doi:10.1016/j.cattod.2004.09.054

reforming, and partial oxidation of methane in a single reactor [7]. The tri-reforming concept represents a new way of thinking both for conversion and utilization of CO_2 in flue gas without CO_2 separation, and for production of industrially useful synthesis gas with desired H_2/CO ratios using flue gas and natural gas. In this paper, the process concept and the experimental results with Ni catalysts are discussed along with computational analysis and kinetic analysis over selected catalysts.

2. Why using flue gas?

The proposed tri-reforming of methane may be carried out using suitable gas mixtures containing CO_2, H_2O, and O_2 as co-feed with natural gas. Based on our research, there appears to be a unique advantage of directly using flue gases, rather than using pre-separated and purified CO_2 from flue gases or other sources, for the tri-reforming process. Flue gases from fossil fuel-based electricity-generating units are the major concentrated CO_2 sources in the US. If CO_2 is to be separated, as much as 100 MW of a typical 500-MW coal-fired power plant would be necessary for today's CO_2 capture processes based on the alkanolamines [4–6]. Therefore, it would be highly desirable if the flue gas mixtures can be used for CO_2 conversion but without pre-separation of CO_2. CO_2 conversion and utilization should be an integral part of CO_2 management, although the amount of CO_2 that can be used for making industrial chemicals is small compared to the quantity of flue gas.

Typical flue gases from natural gas-fired power plants may contain 8–10% CO_2, 18–20% H_2O, 2–3% O_2, and 67–72% N_2; typical flue gases from coal-fired boilers may contain 12–14 vol% CO_2, 8–10 vol% H_2O, 3–5 vol% O_2, and 72–77% N_2. The typical furnace outlet temperature of flue gases is usually around 1200 °C which will decreases gradually along the pathway of heat transfer to produce steam for power generation, while the temperature of the flue gases going to stack is around 150 °C. Pollution control technologies can remove the SO_x, NO_x and particulate matter effectively, but CO_2 and H_2O as well as O_2 remain largely unchanged. When the oxygen-enriched air or oxygen from advanced separation technology is used for combustion in the future, the flue gas will not contain much inert gas N_2 and thus makes the tri-reforming more attractive.

3. Tri-reforming concept

Tri-reforming is a synergetic combination of endothermic CO_2 reforming (Eq. (1)) and steam reforming (Eq. (2)) and exothermic oxidation of methane (Eqs. (3) and (4)). With this process concept, CO_2, H_2O, and O_2 in the flue gas from fossil-fuel-based power plants can be utilized as co-reactants for tri-reforming of natural gas for the production of synthesis gas.

Tri-reforming of natural gas:

$$CH_4 + CO_2 = 2CO + 2H_2[\text{Endothermic} : \Delta H^\circ = 247.3\text{kJ/mol}] \quad (1)$$

$$CH_4 + H_2O = CO + 3H_2[\text{Endothermic} : \Delta H^\circ = 206.3\text{kJ/mol}] \quad (2)$$

$$CH_4 + 1/2O_2 = CO + 2H_2[\text{Exothermic} : \Delta H^\circ = -35.6\text{kJ/mol}] \quad (3)$$

$$CH_4 + 2O_2 = CO_2 + 2H_2O[\text{Exothermic} : \Delta H^\circ = -880\text{kJ/mol}] \quad (4)$$

Reactions for coke formation and destruction:

$$CH_4 = C + 2H_2[\text{Endothermic} : \Delta H^\circ = 74.9\text{kJ/mol}]$$

$$2CO = C + CO_2[\text{Exothermic} : \Delta H^\circ = -172.2\text{kJ/mol}] \quad (6)$$

$$C + CO_2 = 2CO[\text{Endothermic} : \Delta H^\circ = 172.2\text{kJ/mol}] \quad (7)$$

$$C + H_2O = CO + H_2[\text{Endothermic} : \Delta H^\circ = 131.4\text{kJ/mol}] \quad (8)$$

$$C + O_2 = CO_2[\text{Exothermic} : \Delta H^\circ = -393.7\text{kJ/mol}]$$

Fig. 1 illustrates the tri-reforming concept as a new approach to CO_2 conversion using flue gases for synthesis gas (syngas) production. The tri-reforming is a synergetic combination of three catalytic reforming reactions simultaneously in a single reactor. Coupling CO_2 reforming and steam reforming can give syngas with desired H_2/CO ratios for methanol (MeOH) and Fischer–Tropsch (F–T) synthesis. Syngas can be made using natural gas, coal, naphtha, and other carbon-based feedstocks by various processes. Steam reforming of methane, partial oxidation of methane, CO_2 reforming of methane, and autothermal reforming of methane are the representative reaction processes for syngas production from natural gas. The combination of dry reforming with steam reforming can accomplish two important missions: to produce syngas with desired H_2/CO ratios and to mitigate the carbon formation problem that is significant for dry reforming. Integrating steam reforming and partial oxidation with CO_2 reforming could dramatically reduce or eliminate carbon formation on reforming catalyst thus increase catalyst life and process efficiency.

Therefore, the proposed tri-reforming can solve two important problems that are encountered in individual processing. The incorporation of O_2 in the reaction generates heat in situ that can be used to increase energy efficiency and O_2 also reduces or eliminates the carbon formation on the

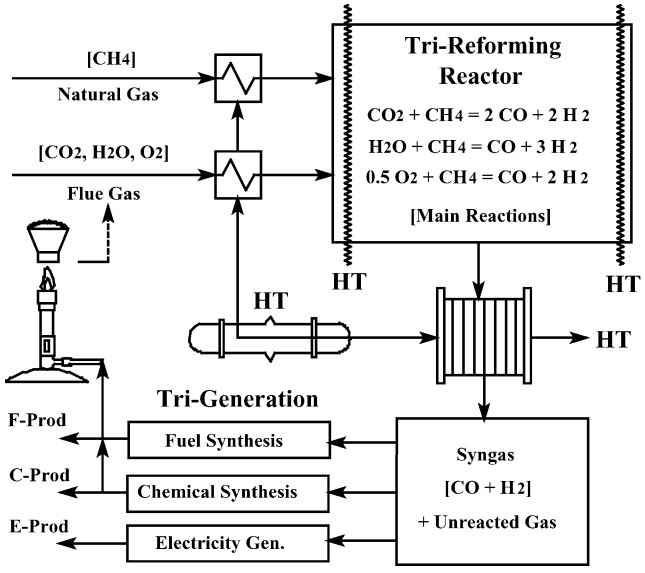

Fig. 1. Process concept for tri-reforming of natural gas using flue gas from fossil fuel-based power plants. HT represents heat transfer or heat exchange including reactor heat up and waste heat utilization.

reforming catalyst. The tri-reforming may be achieved with natural gas and flue gases using the process heat in the power plant and the heat generated in situ from oxidation with the O_2 that is already present in flue gas. This would be more efficient than CO_2 reforming of natural gas. The syngas from tri-reforming can be used for tri-generation of chemicals (such as MeOH and dimethyl ether by oxo-synthesis), ultra-clean fuels (such as liquid hydrocarbons by Fischer–Tropsch synthesis), and electric power (such as electricity by solid oxide fuel cell and molten carbonate fuel cell).

4. Thermodynamics of tri-reforming

Table 1 shows the equilibrium conversions and the product H_2/CO molar ratios calculated using HSC program [10,11] for tri-reforming with various feed gas compositions under atmospheric pressure. Tri-reforming of methane can be carried out with various feed gas compositions, which are not limited to any specific gas mixtures or any power plant flue gases in principle. Table 2 shows the equilibrium conversions of CO_2 and CH_4 for a given type of feed gas composition at different temperatures. As can be seen from Tables 1 and 2, it is possible to perform tri-reforming with over 95% CH_4 conversion and over 80% CO_2 conversion at 800–850 °C when the ratio of CO_2 and H_2O is close to 1.0, $O_2/CH_4 = 0.1$, and the ratio of $(CO_2 + H_2O + O_2)/CH_4 = 1.05$. This is close to the cases with compositions of flue gases.

Figs. 2 and 3 show the effect of the temperature on the equilibrium CH_4 conversion, CO_2 conversion, and H_2/CO ratios, respectively, in the tri-reforming system when the feed gas ratio $(H_2O + CO_2 + 0.5O_2)/CH_4$ (mol ratio) = 1. Tri-reforming can be viewed as a combination of H_2O and O_2 with CO_2 reforming. The combined effects of H_2O and O_2 on the CO_2 reforming can be observed in these figures regarding CO_2 conversion and CH_4 conversion. Considering the CO_2 conversion, the influence of O_2 on CO_2 conversion is much greater, although the effect of H_2O on CO_2 conversion is noticeable. When the gas mixture contains the largest partial pressure of O_2 (e.g., CH_4:CO_2:-H_2O:O_2 = 1:0.25:0.5:0.5) among the studied feed compositions, CO_2 conversion is negative at below 800 °C, suggesting that more CO_2 is actually produced more than consumed. The H_2/CO ratio in the products also strongly depends on the H_2O/CO_2 ratio in the feed while O_2 only has a small effect on H_2/CO ratio, as shown in Fig. 3B.

Fig. 4 shows the equilibrium carbon formation in tri-reforming in comparison with CO_2 reforming. In the proposed tri-reforming, O_2 and H_2O together with CO_2 will be employed to convert natural gas or methane into CO and H_2. It is expected that addition of O_2 and H_2O may reduce carbon formation as encountered in the CO_2 reforming reaction. Based on the thermodynamic analysis, the addition of O_2 can not only suppress the equilibrium carbon formation but also significantly reduce the temperature range (envelope) inside which carbon formation is expected. With the addition of H_2O, H_2O has similar effect on the reduction of equilibrium carbon formation at lower temperatures, while the extent of carbon reduction is not as significant as O_2 at higher temperatures. When both H_2O

Table 1
Equilibrium conversions of CO_2, CH_4, and H_2O, and H_2/CO molar ratios of products for tri-reforming of CH_4 in comparison with CO_2 reforming and H_2O reforming with various CH_4:CO_2:H_2O:O_2 ratios at 850 °C under 1 atm

	CH_4 conversion (%)	CO_2 conversion (%)	Steam conversion (%)	H_2/CO ratio
CH_4:CO_2:H_2O:O_2 = 1:0.475:0.475:0.1	97.9	87.0	77.0	1.67
CH_4:CO_2:H_2O:O_2 = 1:0.45:0.45:0.2	99.0	75.2	56.0	1.69
CH_4:CO_2:H_2O:O_2 = 1:0.375:0.375:0.5	99.8	28.4	−29.0	1.71
CH_4:CO_2:H_2O:O_2 = 1:1:1:0.1	99.8	53.1	26.7	1.48
CH_4:CO_2:H_2O = 1:0:1	94.0	–	95.4	3.06
CH_4:CO_2:H_2O = 1:0.25:0.75	94.9	91.3	93.1	2.25
CH_4:CO_2:H_2O = 1:0.5:0.5	95.8	93.7	88.7	1.66
CH_4:CO_2:H_2O = 1:0.75:0.25	96.6	94.3	76.4	1.32
CH_4:CO_2:H_2O = 1:1:0	97.4	95.0	–	1.03

Table 2
Effect of temperature on equilibrium CO_2 and CH_4 conversions and product H_2/CO molar ratios for tri-reforming of CH_4 with CH_4:CO_2:H_2O:O_2 = 1:0.475:0.475:0.1 at 1 atm

Reaction temperature (°C)	Equilibrium		
	CH_4 conversion (%)	CO_2 conversion (%)	H_2/CO mol ratio
850	97.9	87.0	1.67
800	96.0	81.1	1.72
750	90.7	73.3	1.77
700	86.0	55.6	2.14

and O_2 are used in the CO_2 reforming reaction, as shown in Fig. 4, it is still apparent that O_2 is more effective in reducing equilibrium carbon formation at higher temperatures.

5. Is tri-reforming feasible?

We have not found any previous publications or reports on reforming using flue gases for CO_2 conversion at the time this tri-reforming concept was proposed [7–9]. Our computational analysis shows there are benefits of incorporating steam (H_2O) and oxygen (O_2) simultaneously in CO_2 reforming of CH_4 [10,11]. Prior work established that CO_2 reforming encounters carbon formation problem, even with noble metal catalysts, particularly under elevated pressure [11–13]. Some recent laboratory studies with pure gases have shown that the addition of oxygen to CO_2 reforming [14–17] or the addition of oxygen to steam reforming of CH_4 [18] can have some beneficial effects in terms of improved energy efficiency or synergetic effects in processing and in mitigation of coking. Inui et al. have studied energy-efficient H_2 production by simultaneous catalytic combustion and catalytic CO_2–H_2O reforming of methane using mixture of pure gases including CH_4, CO_2, H_2O, and O_2 [19]. Choudhary and coworkers reported their experimental study on simultaneous steam and CO_2 reforming of methane in the presence of O_2 at atmospheric pressure over Ni/CaO [20,21] or Ni/MgO–SA [22]; they have shown that it is possible to convert methane into syngas with high conversion and high selectivity for both CO and H_2. Ross and coworkers have shown that a Pt/ZrO_2 catalyst is active for steam and CO_2 reforming combined with partial oxidation of methane [23]. Therefore, tri-reforming seems feasible, and we conducted catalytic tri-reforming experiments in a fixed-bed reactor using various catalysts [7–10].

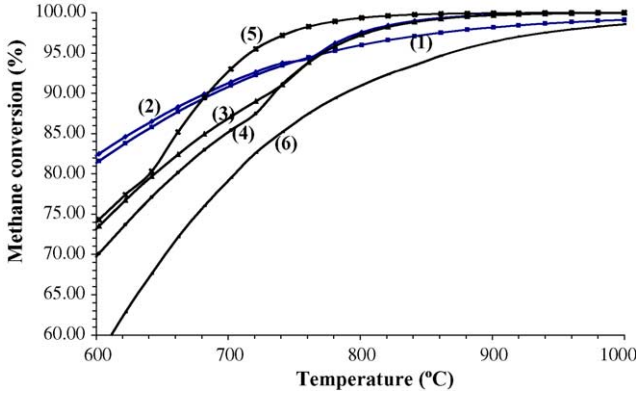

Fig. 2. Equilibrium methane conversion in tri-reforming reaction at atmospheric pressure: (1) CH_4:CO_2:H_2O:O_2 = 1:1:0:0; (2) CH_4:CO_2:H_2O:O_2 = 1:0.9:0:0.2; (3) CH_4:CO_2:H_2O:O_2 = 1:0.45:0.45:0.2; (4) CH_4:CO_2:H_2O:O_2 = 1:0.3:0.6:0.2; (5) CH_4:CO_2:H_2O:O_2 = 1:0.25:0.5:0.5; (6) CH_4:CO_2:H_2O:O_2 = 1:0:1:0.

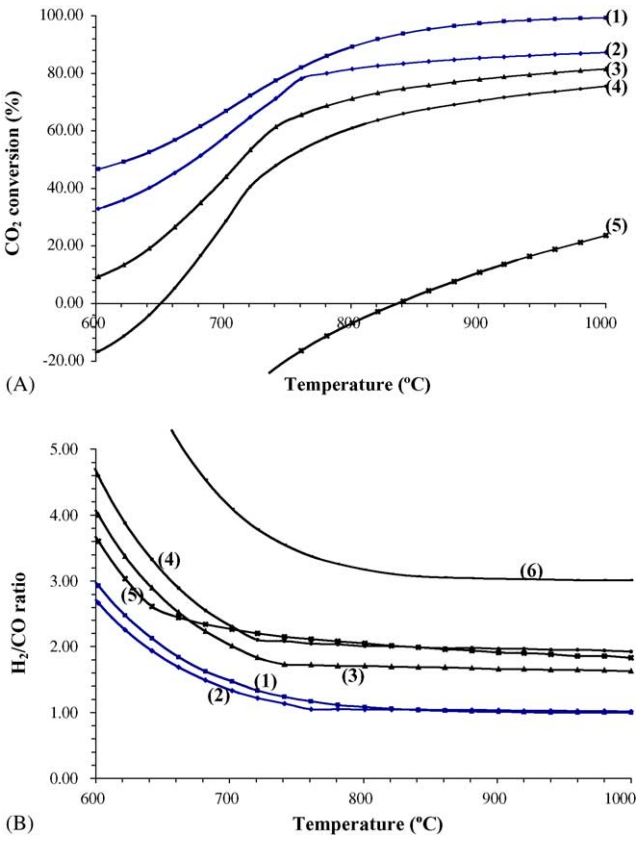

Fig. 3. (A) Equilibrium CO_2 conversion in tri-reforming reaction at atmospheric pressure: (1) CH_4:CO_2:H_2O:O_2 = 1:1:0:0; (2) CH_4:CO_2:H_2O:O_2 = 1:0.9:0:0.2; (3) CH_4:CO_2:H_2O:O_2 = 1:0.45:0.45:0.2; (4) CH_4:CO_2:H_2O:O_2 = 1:0.3:0.6:0.2; (5) CH_4:CO_2:H_2O:O_2 = 1:0.25:0.5:0.5. (B) Equilibrium H_2/CO ratio in tri-reforming reaction at atmospheric pressure: (1) CH_4:CO_2:H_2O:O_2 = 1:1:0:0; (2) CH_4:CO_2:H_2O:O_2 = 1:0.9:0:0.2; (3) CH_4:CO_2:H_2O:O_2 = 1:0.45:0.45:0.2; (4) CH_4:CO_2:H_2O:O_2 = 1:0.3:0.6:0.2; (5) CH_4:CO_2:H_2O:O_2 = 1:0.25:0.5:0.5; (6) CH_4:CO_2:H_2O:O_2 = 1:0:1:0.

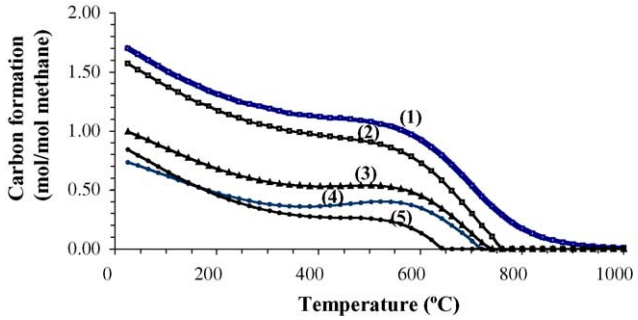

Fig. 4. Equilibrium carbon formation in tri-reforming reaction at different feed compositions at atmospheric pressure. (1) CH_4:CO_2:H_2O:O_2 = 1:1:0:0; (2) CH_4:CO_2:H_2O:O_2 = 1:0.9:0:0.2; (3) CH_4:CO_2:H_2O:O_2 = 1:0.45:0.45:0.2; (4) CH_4:CO_2:H_2O:O_2 = 1:0.3:0.6:0.2; (5) CH_4:CO_2:H_2O:O_2 = 1:0.25:0.5:0.5. (All ratios are mol ratios.)

6. Tri-reforming catalyst preparation and characterization

6.1. Catalyst preparation

Various supported Ni catalysts were prepared in our laboratory for tri-reforming in the present work. The supports include CeO_2, ZrO_2, MgO, Al_2O_3, and the mixed oxide of Ce and Zr (denoted as CeZrO with Ce:Zr atomic ratio of 3) prepared using the soft chemistry technique reported by Rossigonol et al. [24] with $Ce(NO_3)_3{\cdot}6H_2O$ and $Zr(OCH_2CH_2CH_3)_4$ as the precursors. Ni was dispersed on these supports by wet impregnation method using nickel nitrate $Ni(NO_3)_2{\cdot}6H_2O$ under agitation for 1 h, followed by drying in the oven at 60 °C overnight. The dried solid was ground into power and then calcined at 870 °C for 6 h in air. The Ni/MgO/CeZrO catalyst was prepared by the same procedures as described above except $Mg(NO_3)_2{\cdot}6H_2O$ (99% purity) was used as the precursor of MgO and both $Ni(NO_3)_2{\cdot}6H_2O$ and $Mg(NO_3)_2{\cdot}6H_2O$ were dissolved into 4 ml distilled H_2O to form an aqueous solution. The weight percentage of MgO in the Ni/MgO/CeZrO catalyst was ca. 10 wt.%. A commercial Al_2O_3 catalyst (ICI Synetix 23-4, R15513) was also tested for comparison.

The supports were selected based on the following considerations: supports with basic properties or high oxygen storage properties may promote the adsorption of CO_2 on catalysts and, consequently, enhance the CO_2 conversion. Based on a simplified mechanism of CO_2 conversion in the CO_2 reforming reaction [25–27], the reaction starts from the activation of methane followed by the surface reaction with surface CO_2 species or adsorbed oxygen atoms derived from CO_2 ($CO_2 + * = CO + O^*$, * denotes an active site). Compared with H_2O and O_2, CO_2 is more acidic. Basic supports may preferentially interact more strongly with CO_2 than H_2O and O_2. Once CO_2 is adsorbed on the catalyst surface, it may have more chance to react with CH_4 and form CO and H_2. Similarly, supports with more oxygen storage capacity may facilitate the dissociative adsorption of CO_2 into CO and adsorbed oxygen by $CO_2 + * = CO + O^*$, leading to the enhanced conversion of CO_2. MgO is a basic support which has been reported for CO_2 reforming [28–31], steam reforming [32,33], and methane partial oxidation [34]. However, no reports have been found on the comparison of CO_2 conversion in the presence of H_2O and O_2 as in the tri-reforming process. The mixed oxide of Ce and Zr has been reported to have a larger oxygen storage capacity although the oxygen storage capacity of CeO_2 and ZrO_2 themselves is very little [24]. The application of this material has not yet been studied in tri-reforming, although similar support material has been tested by Roh et al. [32] in oxy-steam reforming. CeO_2 and ZrO_2 were chosen as supports for the purpose of comparison.

6.2. Catalyst characterization

Table 3 lists the physical properties and composition of the supported Ni catalysts and their corresponding supports characterized by the BET (using Quartchrome Autosorb-1 unit) and ICP–MS (using Finnigan Element 1 instrument). The surface area was measured by both single-point BET

Table 3
Properties of supported nickel catalysts prepared for tri-reforming

Catalysts	Ni loading (wt.%) by ICP–MS	Specific surface area by single point BET method (m^2/g)	Specific surface area by multipoint BET method (m^2/g)	Average Ni particle size by XRD (nm)
Ni/CeO_2	5.5	2.2	1.2	84.9
Ni/ZrO_2	3.8	5.5	7.4	43.9
Ni/CeZrO	6.0	16.5	28.9	16.4
Ni/MgO	8.0	16.8	26.1	n.d.
Ni/MgO/CeZrO	6.3	14.0	23.3	n.d.
ICI I15513 (Ni/Al_2O_3)		3.4	4.4	44.1
CeO_2	n.a	1.6		n.a.
ZrO_2	n.a	5.5		n.a.
CeZrO	Ce/Zr (atomic ratio = 4.4)	20.6		
MgO	n.a	28.4		n.a.

n.d.: Not detectable; n.a.: not applicable.

method (conducted at $P/P_0 = 0.3$) and multipoint BET method. The surface area of the selected supports decreases in the order of MgO ≈ CeZrO > ZrO_2 > CeO_2. It is interesting to notice that CeZrO has much higher surface area than its components, CeO_2, and ZrO_2, indicating that CeZrO is not a mechanical mixture of CeO_2 and ZrO_2. After Ni loading, the surface area of the prepared catalysts has no significant change. The ICP analysis shows that the Ni loading on these catalysts is around 6.0% except Ni/MgO, which has a higher loading (8.0 wt.%) and Ni/ZrO_2, which has a lower loading (3.8 wt.%). All the prepared Ni catalysts are meso-porous or non-porous materials and have small pore volume, as indicated by their isotherm adsorption and desorption curves.

Fig. 5 shows the XRD patterns of reduced Ni/Al_2O_3 and Ni/MgO before and after reduction (reduced at 100 °C for 10 min, 450 °C for 75 min, and 850 °C for 10 min under H_2 flow) (measured using Scintag Pad V-242 XRD instrument). Over Ni/MgO, only diffraction peaks of MgO at 2θ of 36.9°, 42.9°, 62.3°, 74.7°, and 78.6° are found, no matter whether this catalyst is reduced or not. No separate peaks assigned to NiO can be identified, even though the diffraction peaks of NiO (2θ = 37.2°, 43.3°, 62.9°, 75.4°, and 79.4°) are very close to those of MgO. The absence of NiO diffraction peaks in NiO/MgO indicates the formation of NiO/MgO solid solution [35,36,37]. Ni and Mg cations have similar ironic radii (ca. 0.78 Å), the same oxidation state (2+), and the same NaCl-type cubic bulk oxide structure. Based on Hume–Rothery criteria [38], NiO and MgO are very likely to form an extensive solid solution. On the other hand, well-identified Ni particle crystallite diffraction peaks at 2θ of 44.5°, 51.8°, and 76.4° are observed over Ni/Al_2O_3 (ICI) catalyst reduced at 850 °C, indicating large Ni particles were formed on Al_2O_3. This is confirmed by the BSE (back-scattered electrons)-SEM image of the same reduced catalyst shown in Fig. 6. The white spots in the BSE-SEM image are Ni particles, which is confirmed by the elemental analysis of these white spots. The presence of Al in the elemental analysis of the white spots is because the elemental analysis by EDS (energy dispersive X-ray spectroscopy) has a minimum measurement area of 1 μm × 1 μm which is larger than the Ni particles over the catalyst. Hence, the Al signal may result from Al in the support. The elemental analysis at an area without white spots shows that there is no Ni present, further confirming that white spots are particles containing Ni. From Fig. 6, it is

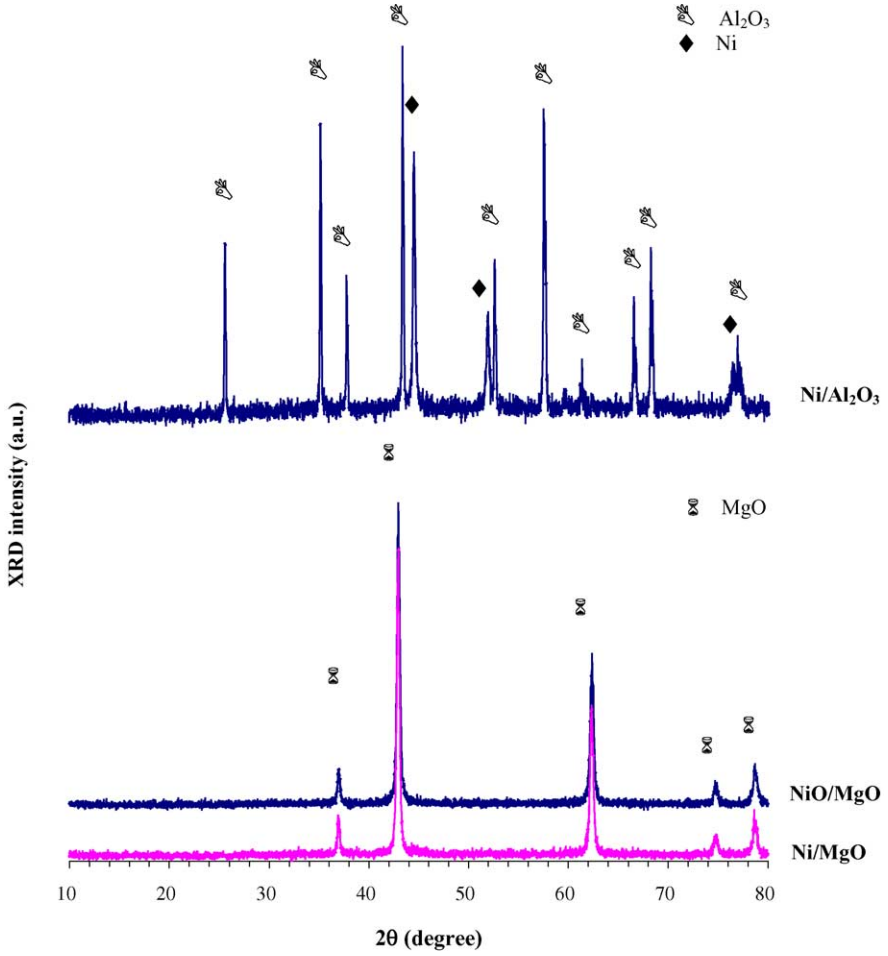

Fig. 5. XRD pattern of reduced Ni/Al_2O_3 and Ni/MgO before and after reaction. (Reduced at 100 °C for 10 min, 450 °C for 75 min, and 850 °C for 10 min under H_2 flow.)

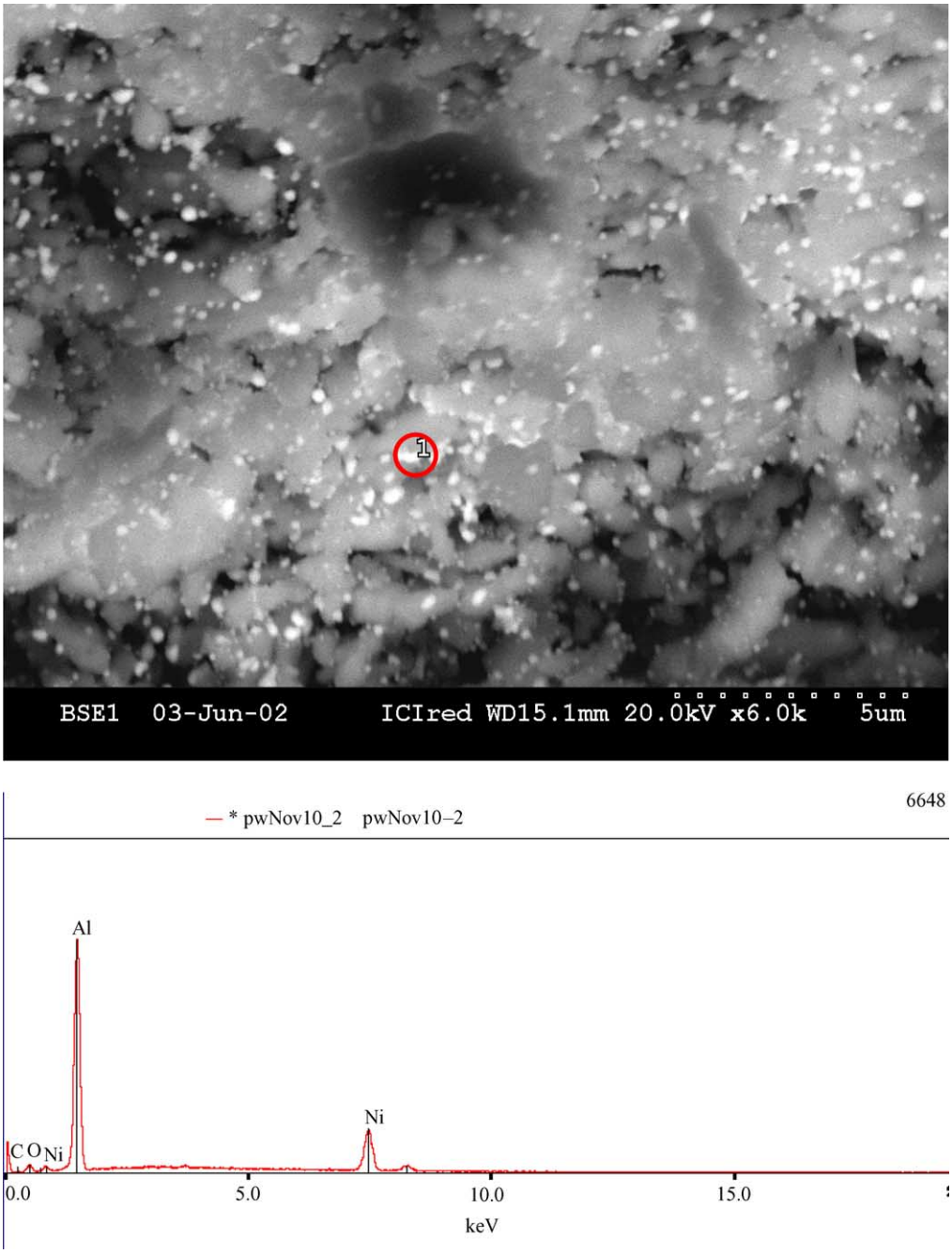

Fig. 6. BSE (backscattered electrons)-SEM image of reduced Ni/Al_2O_3 (ICI) catalyst and the elemental analysis by EDS of a bright spot in the BSE-SEM image.

found, however, that the size of Ni particles is widely distributed, ranging from 300 to 400 nm to less than 50 nm.

Figs. 7 and 8 show the XRD patterns of the CeO_2- and ZrO_2- and mixed oxide-supported Ni catalysts before and after reduction. In the case of Ni/CeO_2, Ni/ZrO_2, and Ni/CeZrO, NiO diffraction peaks at 2θ of 37.2°, 43.3°, and 62.9° are identified before reduction. After reduction, NiO diffraction peaks disappear and Ni diffraction peaks become visible. Two different forms of ZrO_2 are observed in the Ni/ZrO_2 catalyst. Most of the ZrO_2 is in the tetragonal form. Only a small amount of ZrO_2 is in the form of the monoclinic phase. Monoclinic and tetragonal structures are the most common crystalline forms of ZrO_2 and two of them are often found together [24]. Even after the reduction at 850 °C, tetragonal ZrO_2 is still the predominant form, suggesting that the tetragonal phase is stable under the conditions employed. At the calcination temperature higher than 1000 °C, ZrO_2 has been found to consist of a pure monoclinic phase [24]. The XRD spectrum of CeZrO in the Ni/CeZrO catalyst shows that CeZrO has much broader

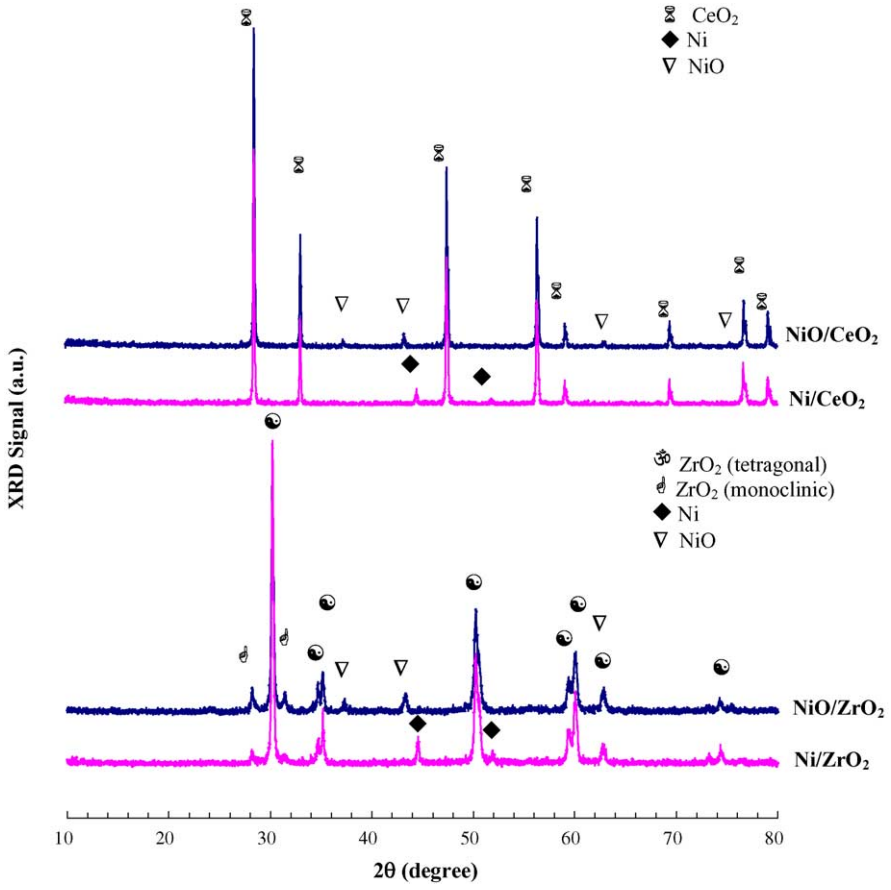

Fig. 7. XRD pattern of Ni/CeO_2 and Ni/ZrO_2 before and after reduction. (Reduced at 100 °C for 10 min, 450 °C for 75 min, and 850 °C for 10 min under H_2 flow.)

diffraction peaks and is different from those of CeO_2 and ZrO_2. The diffraction peaks of CeZrO suggest that CeZrO is in the form of $Ce_{0.75}Zr_{0.25}O_2$, the form of which is reported to have higher oxygen storage capacity (OSC) [24]. The structure of $Ce_{0.75}Zr_{0.25}O_2$ in the Ni/CeZrO catalyst is suggested to be stable by comparing the XRD spectra of Ni/CeZrO before and after reduction. The higher OSC of this material may be due to the increased oxygen mobility resulting from the introduction of small amounts of zirconium in the ceria structure [39], which is supported by the following TPR and CO_2-TPD results.

In the Ni/MgO/CeZrO catalyst (Fig. 8), $Ce_{0.75}Zr_{0.25}O_2$ is again identified. However, except the diffraction peaks from MgO, no diffraction peaks from NiO and Ni were found over this catalyst before and after its reduction. This phenomenon is also observed over Ni/MgO (Fig. 5).

Due to the formation of a NiO/MgO solid solution, NiO is very difficult to reduce in the NiO/MgO solid solution as evidenced by the TPR of Ni/MgO (see below). Even if some NiO in the solid solution is reducible at higher temperatures, highly dispersed Ni would be expected. As a result, no Ni diffraction peaks appeared in the XRD spectrum of the reduced Ni/MgO. This also explains the absence of Ni diffraction peaks in the XRD spectrum of the reduced Ni/MgO/CeZrO catalyst.

Since crystalline Ni is found in the reduced Ni/Al_2O_3 (ICI), Ni/ZrO_2, Ni/CeO_2, and Ni/CeZrO, the diffraction peak of Ni (1 1 1) at 2θ of 44.5° was again acquired by slow scans over the range of 43.6–46° 2θ and used to calculate the average Ni particle size using the Scherrer equation [40], in which the wavelength is 0.154 nm and the Scherrer constant is 0.9. The calculated Ni particle size is listed in Table 3. Ni over Ni/CeO_2 shows the highest average particle size (ca. 85 nm). The average size of Ni over CeZrO is about 16.4 nm, while Ni on ZrO_2 and Al_2O_3 has similar average size of 44 nm. It should be noted that the particle size estimated from the Ni XRD diffraction peak is an average value of Ni particles on the reduced Ni/Al_2O_3 except those small Ni particles (e.g., <10 nm) which may be transparent to XRD. Theoretically the average Ni particle size could also be estimated from the particle size distribution from the SEM image of the reduced Ni/Al_2O_3, provided that the particle size distribution can be obtained from the SEM image [41]. However, due to the low resolution of the BSE-SEM, small particles (e.g., <10 nm) cannot be measured accurately either. Therefore, both XRD and SEM are not a reliable technique to measure Ni particle size when there are small particles (e.g., <10 nm) on the catalyst.

H_2 pulse chemisorption has also been conducted (using Micromeritics AutoChem 2910) to determine the Ni particle

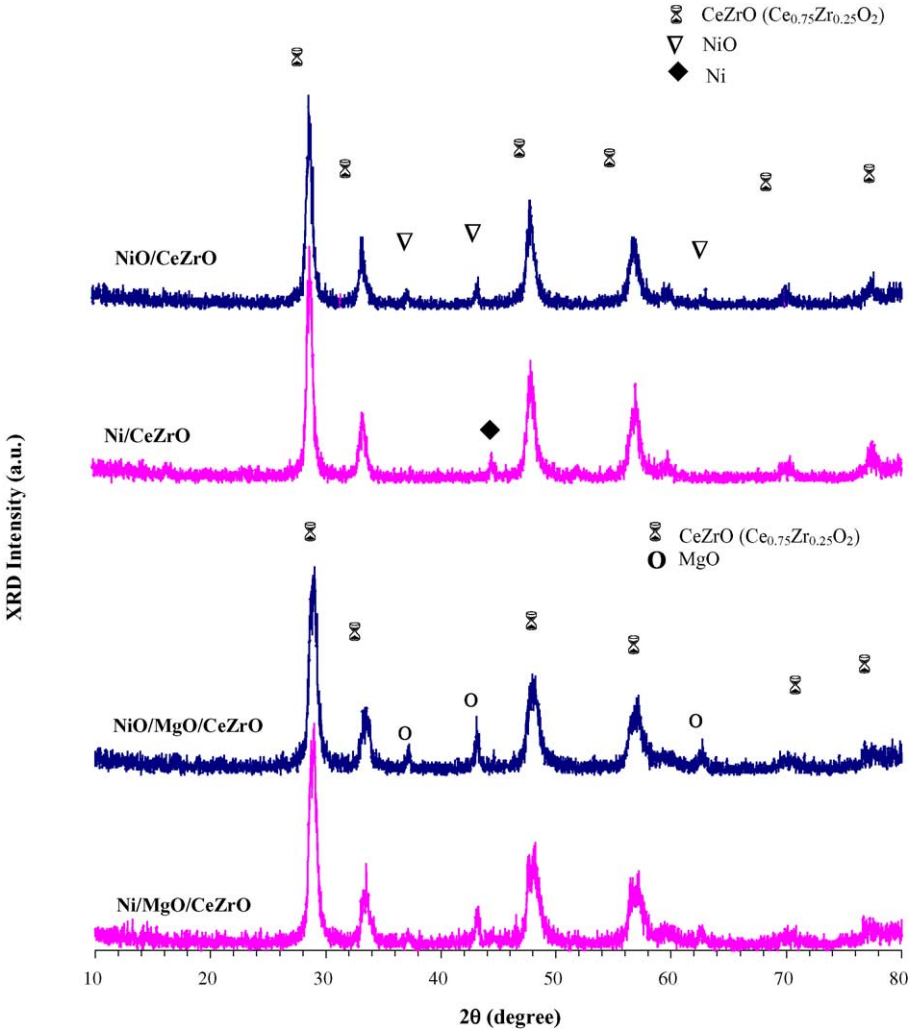

Fig. 8. XRD pattern of Ni/CeZrO and Ni/MgO/CeZrO before and after reduction. (Reduced at 100 °C for 10 min, 450 °C for 75 min, and 850 °C for 10 min under H_2 flow.)

size on the reduced Ni catalysts. However, due to the large Ni particles and small amount of samples available, the chemsorption of H_2 is very small on these samples, which makes it difficult to accurately determine the Ni particle size by this method. In the case of the reduced Ni/MgO and Ni/MgO/CeZrO samples, the small Ni particle size is expected because no Ni crystalline diffraction peaks are observed in their XRD spectra. However, it is noticed that only a small amount of Ni in Ni/MgO and Ni/MgO/CeZrO is reduced at 850 °C according to their TPR profiles. The uncertainty of the extent of the reduction of Ni in these catalysts makes it more difficult to determine particle size by the chemisorption technique.

6.3. Temperature programmed reduction (TPR)

As shown by TPR profiles in Fig. 9 (measured using Micromeritics AutoChem 2910 TPR), ZrO_2 itself is not reducible at temperatures below 850 °C. CeO_2, however, becomes reducible at 600 °C. The extent of its reduction gradually increases with the increasing temperatures up to the maximum experimental temperature (850 °C), indicating that CeO_2 is only partially reduced up to 850 °C. This partial reducibility of CeO_2 rationalizes why CeO_2 shows a

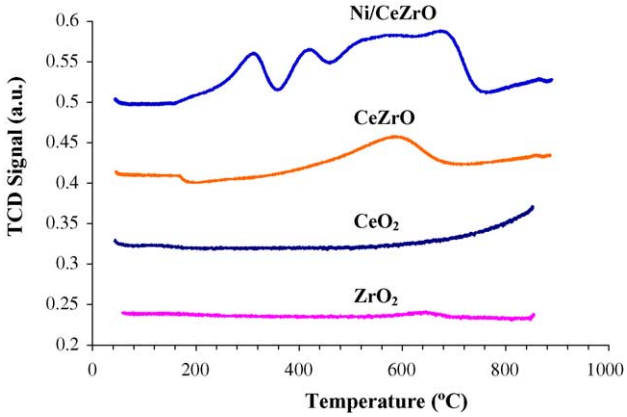

Fig. 9. TPR profiles on ZrO_2, CeO_2, CeZrO (Ce–Zr oxide mixture), and Ni supported on CeZrO.

redox behavior [39] and a catalytic reactivity in oxidation reaction [42]. Different from CeO_2, the prepared mixed oxide of Ce and Zr, CeZrO, shows a broad reduction peak in the range 220–660 °C, with the peak position at 611 °C and a reduction tail at temperature higher than 660 °C. It is reported that the addition of ZrO_2 to CeO_2 can facilitate the reduction of CeO_2 and enhance the oxygen storage capacity [39]. The TPR profile of NiO/CeZrO shows more complicated patterns. Two reduction peaks at 322 and 429 °C are probably related to the reduction of isolated NiO, having different extent of interaction with the support [43]. The tailing at the temperature above 770 °C is similar to that in the TPR of CeZrO itself. The broad peak in the range of 470 and 770 °C cannot be identified unambiguously. It probably corresponds to the reduction of both Ni and Ce species in the NiO/CeZrO catalyst.

Fig. 10 compares TPR profiles of Ni catalysts supported on different supports. Ni/Al_2O_3 (ICI) has a major peak at 490 °C due to the reduction of NiO. There are two reduction peaks over Ni/ZrO_2 at 464 and 556 °C, respectively, similar to the observation by Roh et al. [43]. Over Ni/CeO_2, a major reduction peak at 426 °C is observed. This reduction peak temperature is lower than those over NiO/ZrO_2, suggesting that the interaction between NiO and CeO_2 is weaker than that between NiO and ZrO_2. This may explain why the average Ni particle size on CeO_2 is larger than that on ZrO_2 (Table 3) after both catalysts were reduced at 850 °C. The small and broad reduction peak at 590 °C over Ni/CeO_2 cannot be assigned to a specific species. Based on the TPR of CeO_2 itself, CeO_2 starts to be reducible at the temperature close to 590 °C. In addition, the presence of Ni may enhance the reducibility of CeO_2, as evidenced by the difference of CO_2-TPD of CeO_2 and Ni/CeO_2 (see below). However, it does not exclude the possibility that some of NiO may be reduced at this temperature as well. The tailing at high temperatures over Ni/CeO_2 is similar to the reduction pattern of CeO_2 itself.

Over Ni/MgO/CeZrO, one small reduction peak at 380 °C is observed, suggesting the existence of small amount of isolated NiO. The absence of NiO diffraction peaks from the XRD spectrum of Ni/MgO/CeZrO is probably because the amount of the isolated NiO is too small to be picked up by XRD measurement. The tailing of reduction starting from 560 °C over Ni/MgO/CeZrO is probably similar to that on the Ni/CeZrO catalyst. Compared with the TPR profile of the Ni/CeZrO catalyst, it is suggested that most of the NiO in the Ni/MgO/CeZrO has not be reduced at the temperature below 850 °C.

Over Ni/MgO, no obvious reduction peak is found although a small amount of reduction at high temperature is observable when the Ni/MgO reduction profile is expanded as shown in Fig. 11. Therefore, it is highly likely that no isolated NiO is present in NiO/MgO and almost all the NiO has formed a solid solution with MgO. NiO in NiO/MgO solid solution was reported to be difficult to reduce [35]. Based on this finding, it is suggested that most of the NiO in Ni/MgO/CeZrO form a solid solution with MgO as well.

The TPR results are generally consistent with the observations by the XRD. NiO over Al_2O_3, CeO_2, ZrO_2, and CeZrO is reducible below 850 °C, even though the extent of interactions is different between NiO and these supports. Therefore, NiO and Ni XRD diffraction peaks were observed over these catalysts before and after reduction. The absence of NiO and Ni from the XRD spectra over Ni/MgO/CeZrO and Ni/MgO catalysts is due to the formation of NiO/MgO solid solution.

6.4. CO_2-TPD

CO_2-TPD was conducted (using Micromeritics AutoChem 2910 TPD) to investigate the interaction of CO_2 with the prepared supported Ni catalysts (Fig. 12). Over Ni/Al_2O_3 (ICI catalyst), there is almost no CO_2 desorption from this catalyst, indicating that neither Ni nor Al_2O_3 has a strong interaction with CO_2. Over Ni/ZrO_2, a small and broad CO_2 desorption peak is observed in the range 100–405 °C with the peak position at 137 °C. A well-defined desorption peak at 740 °C is found over Ni/CeO_2 catalyst. Ni/MgO, Ni/CeZrO, and Ni/MgO/CeZrO all show large CO_2 desorption peaks, except that Ni/MgO has a much broader peak, from

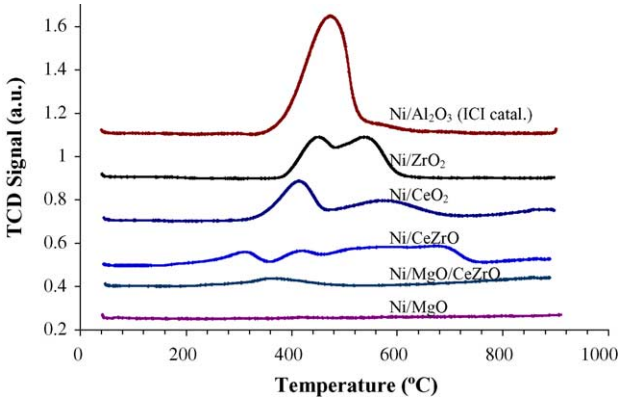

Fig. 10. TPR over Ni catalysts supported on different supports.

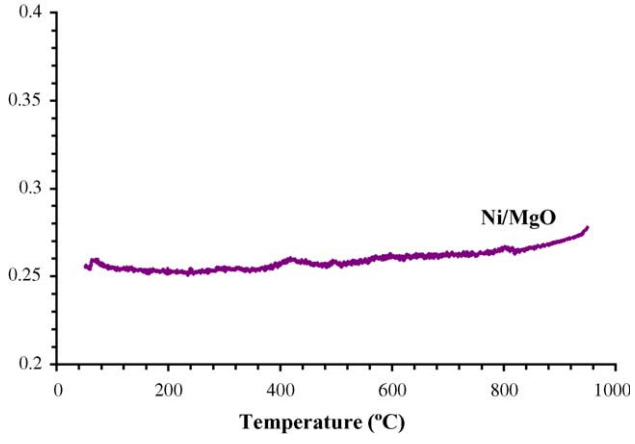

Fig. 11. Expanded TPR profile for Ni/MgO.

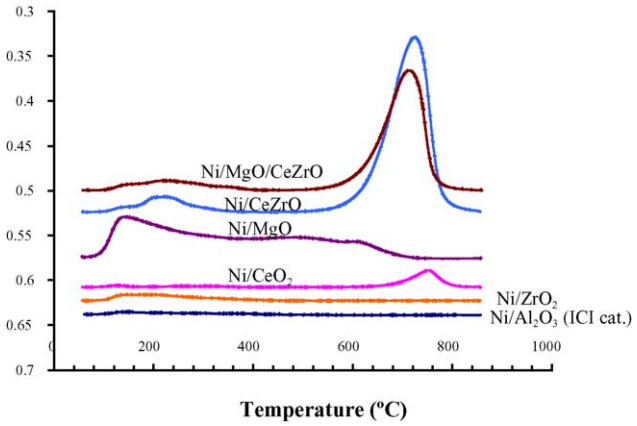

Fig. 12. CO_2-TPD over supported Ni catalysts.

85 to 714 °C. Ni/MgO/CeZrO and Ni/CeZrO have similar pattern of CO_2-TPD profiles with major desorption peak at 710–717 °C. Based on these TPD results, it is clear that Ni/MgO, Ni/MgO/CeZrO, and Ni/CeZrO have the property expected from the design of these catalysts. Catalysts employing MgO or CeZrO as supports show more and stronger interaction with CO_2.

The CO_2 desorption profile over Ni/MgO is very similar to that over its support, MgO, indicating that CO_2 adsorption mostly takes place on the MgO support (Fig. 13). Interestingly, different CO_2-TPD profiles are observed over Ni/CeZrO, Ni/CeO_2, and their supports. Over CeO_2, almost no CO_2 desorption is observed. However, a small but well defined desorption peak at 740 °C is found over Ni/CeO_2. This is probably related to the presence of Ni. Ni metals may promote the reduction of CeO_2 and create more oxygen vacancy in CeO_2 during the reduction, resulting in new sites for CO_2 adsorption. This speculation is partly supported by comparing the TPR profiles of CeO_2 and Ni/CeO_2. The broad reduction peak at 590 °C over Ni/CeO_2 may include the reduction of CeO_2 under the assistance of Ni metal. The TPD profiles of CeZrO and Ni/CeZrO are also very different. Over CeZrO, there is a large CO_2 desorption peak at 380 °C.

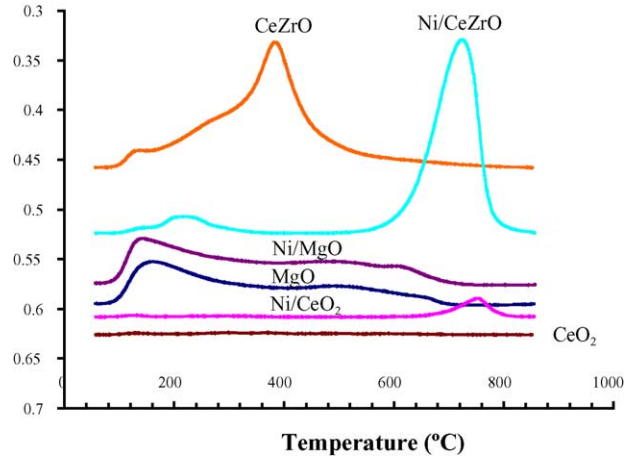

Fig. 13. CO_2-TPD over supports and supported Ni catalysts.

In the case of Ni/CeZrO, a major CO_2 desorption peak at 717 °C is observed with a small amount of CO_2 desorption in a lower temperature range. The position of this major CO_2 desorption peak is similar to that observed over Ni/CeO_2. Again, this shift of CO_2 desorption temperatures over CeZrO and Ni/CeZrO may be related to the presence of Ni. However, it is not clear at present stage whether Ni directly takes part in the CO_2 adsorption over these catalysts or Ni has an indirect effect on the structure of CeZrO during the reduction. Further exploration is necessary to clarify this issue.

7. Catalytic tri-reforming reactions

7.1. Tri-reforming over the Ni/MgO/CeZrO catalyst

It should be noted that tri-reforming is a catalytic process under the conditions employed (1 atm and 700–850 °C). Without a catalyst, almost no reaction (<0.01% methane conversion) was observed in tri-reforming, even at 850 °C. The catalytic activity test was conducted at 1 atm in a fixed-bed quartz reactor (i.d. = 4 mm) interfaced with a flow-controlling system and an on-line gas chromatograph (SRI GC equipped with a TCD). Two packed GC columns, Silica Gel and Molecular Sieve 5A, were used for the complete separation of H_2, O_2, CH_4, CO and CO_2. In all the analyses, H_2O was condensed before gases in the products were analyzed by the GC. Prior to each experiment, about 100 mg of a catalyst (18–35 mesh) was loaded into the quartz reactor supported by quartz wool and positioned in the isothermal zone of the furnace. The catalyst was reduced using 25% H_2 in Ar (5 ml/min H_2 + 15 ml/min Ar) at 100 °C for 10 min, 450 °C for 75 min, and 850 °C for 10 min. The heating rate was 12 °C/min from room temperature to 100 °C, from 100 to 450 °C, and from 450 to 850 °C. After the reduction, the catalyst was purged with Ar (15 ml/min) for 10 min at 850 °C and reactant gas mixtures were prepared in another line. The compositions of the gas mixtures were controlled by the flow rate of each gas. The prepared gas mixtures were then switched back into the reactor. The distilled H_2O was pumped into the reactor 3–5 min using a pulse-free HPLC pump before the pre-mixed gas reactants were switched into the reactor in order to prevent carbon formation due to the absence of H_2O. However, when the catalyst was Ni/MgO, it was found that introduction of H_2O before the gas reactants may cause the complete deactivation of this catalyst. Therefore, the gas reactants were introduced into the reactor 3–5 min before the introduction of H_2O in the case of Ni/MgO catalyst. After the reaction stabilized for 0.5–1 h, the reaction products were analyzed by the GC every half hour.

The conversion of CH_4 and CO_2 in tri-reforming was calculated as follows:

CH_4 conversion = 1 − [mole no. of CH_4 in the product]/[mole no. of CH_4 in the feed]

CO_2 conversion = 1 − [mole no. of CO_2 in the product]/[mole no. of CO_2 in the feed]

Since the reactants in tri-reforming contain CH_4, CO_2, H_2O, O_2 and the only products from tri-reforming are CO and H_2, the selectivity to CO and H_2 will be essentially 100%. Therefore, the ratio of H_2/CO in the products becomes more useful parameter.

The calculations for the yields of CO and H_2 are somewhat more complicated but can be done by the following equations: CO yield = [measured mole no. of CO in the products]/[theoretical mole no. of CO in the products based on CH_4 and CO_2]; H_2 yield = [measured mole no. of H_2 in the products]/[theoretical mole no. of H_2 in the products based on CH_4 and H_2O]. The theoretical ratio of the products depends on the feed compositions, because the system involves multiple reactions simultaneously: $CH_4 + (xCO_2 + yH_2O + zO_2) = mCO + nH_2$ where the products are controlled by the feed gas ratios among CO_2, H_2O, O_2, and CH_4. If the sum of $xCO_2 + yH_2O + zO_2$ equals to the number of moles of CH_4 by stoichiometry of chemical reactions, the yield equations can be written as follows: CO yield = [measured mole no. of CO in the products]/[(mole no. of CH_4) + (mole no. of CO_2)]; H_2 yield = [measured mole no. of H_2 in the products]/[2 × (mole no. of CH_4) + (mole no. of H_2O)]. If CO_2 or H_2O or O_2 is oversupplied, a simple equation cannot be written without calculating the theoretical mole no. of H_2 or CO in the products by considering multiple reactions involving CH_4. Because of the above equations, the yield ratio of H_2 and CO does not equal to the molar ratios of H_2 and CO. Therefore, to avoid confusion, we will use H_2/CO product molar ratio, instead of H_2 yield or CO yield, in subsequent results and discussions.

Two sets of tri-reforming experiments were conducted at 850 °C and 1 atm over Ni/MgO/CeZrO in a fixed-bed quartz flow reactor. These tests were run in order to elucidate the effect of H_2O and O_2 in the feed on tri-reforming. In the first set of experiments, O_2/CH_4 and $(H_2O + CO_2 + O_2)/CH_4$ (mol ratio) were kept at 0.1 and 1.03, respectively, except the ratio of H_2O/CO_2 changed. In the other set, H_2O/CO_2 and $(H_2O + CO_2 + 2O_2)/CH_4$ (mol ratio) in the feed were kept constant at 1 and 1.2, respectively, while changing the O_2/CH_4 ratio. The experimental results of these two sets of experiments together with the equilibrium data are shown in Figs. 14 and 15.

At the space velocity of ca. 32,000 ml/(h g cat.), tri-reforming is found to be close to equilibrium in all the experiments over the Ni/MgO/CeZrO catalyst. The trend of CH_4 conversion, CO_2 conversion, and H_2/CO ratio at different feed compositions is consistent with the prediction by the thermodynamic analysis.

For example, in the first set experiments (Fig. 14), CH_4 conversions are almost unchanged in the range of 91–93% (equilibrium CH_4 conversion is about 98–99%). H_2/CO ratios drop from 2.88 (equilibrium: 3.03) at CH_4:H_2O:CO_2:O_2 (mol ratio) = 1:1.03:0:0.1 to 2.08 (equilibrium: 2.30) at CH_4:H_2O:CO_2:O_2 = 1:0.81:0.21:0.1 and further to 1.19 (equilibrium: 1.29) at CH_4:H_2O:CO_2:O_2 = 1:0.28:0.75:0.1. CO_2 conversions have the opposite trend. At CH_4:H_2O:CO_2:O_2 = 1:0.81:0.21:0.1, CO_2 conversion is only about 55.8% (equilibrium: 67.6%), while it increases to 73.5% (equilibrium: 81.3%) and 80.1% (equilibrium: 86.3%), respectively, when H_2O/CO_2 mol ratio decreases to 0.56/0.48 and 0.28/0.75.

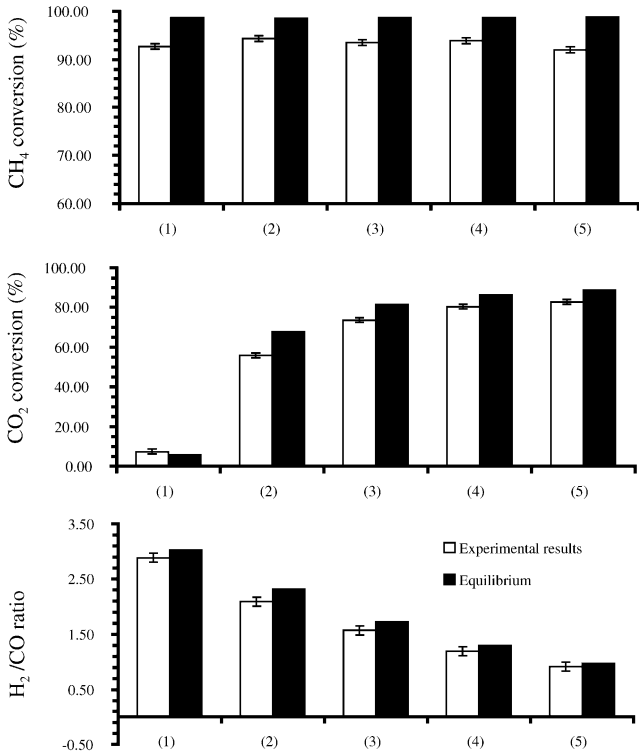

Fig. 14. Comparison of equilibrium CH_4 conversion, CO_2 conversion, and H_2/CO ratio in the tri-reforming and experimental CH_4 conversion, CO_2 conversion, and H_2/CO ratio over 100 mg Ni/MgO/CeZrO at 1 atm and 850 °C at different gas compositions: (1) CH_4:H_2O:CO_2:O_2 = 1:1.03:0:0.1; (2) CH_4:H_2O:CO_2:O_2 = 1:0.81:0.21:0.1; (3) CH_4:H_2O:CO_2:O_2 = 1:0.56:0.48:0.1; (4) CH_4:H_2O:CO_2:O_2 = 1:0.28:0.75:0.1; (5) CH_4:H_2O:CO_2:O_2 = 1:0:1.03:0.1. (All the ratios are mol ratios; CH_4 flow rate = 25 ml/min.)

Fig. 15 shows the tri-reforming reaction at different O_2 concentrations at the fixed ratio of H_2O/CO_2 = 1 and $(H_2O + CO_2 + 2O_2)/CH_4$ = 1.2. The H_2/CO ratio in the product is almost unchanged in the range 1.52–1.60 (equilibrium: 1.62–1.79) when feed changes from CH_4:H_2O:CO_2:O_2 = 1:0.6:0.6:0 to CH_4:H_2O:CO_2:O_2 = 1:0.27:0.27:0.33. The improvement of CH_4 conversions from 89.4 to 96.5% is observed even though the equilibrium CH_4 conversions are always above 98% under these conditions. This implies that the addition of a certain amount of O_2 can improve the activity over a catalyst. The decrease of CO_2 conversion is also observed when more oxygen is contained in the feed. The CO_2 conversion drops from 78.4% (equilibrium: 86.6%) at CH_4:H_2O:CO_2:O_2 = 1:0.6:0.6:0 to 67.8% (equilibrium: 72.7%) at CH_4:H_2O:CO_2:O_2 = 1:0.27:0.27:0.33.

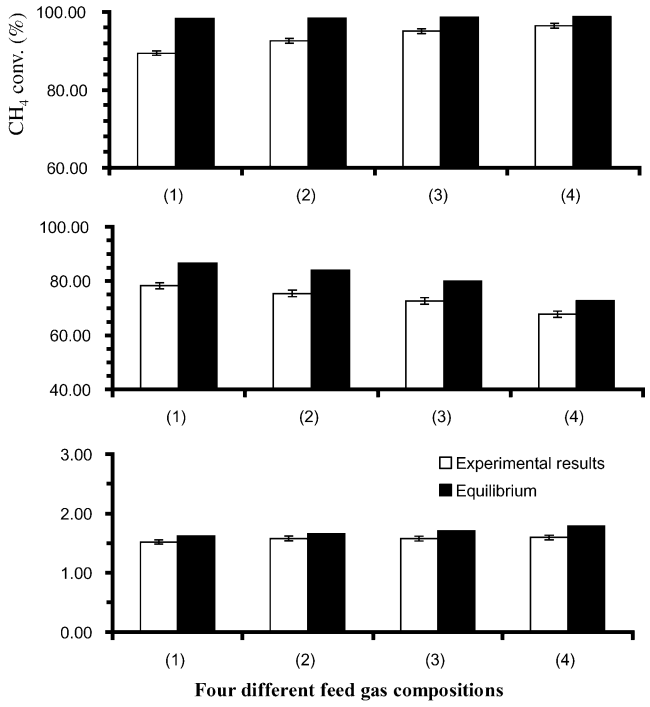

Fig. 15. Comparison of equilibrium CH_4 conversion, CO_2 conversion, and H_2/CO ratio in the tri-reforming and experimental CH_4 conversion, CO_2 conversion, and H_2/CO ratio over 100 mg Ni/MgO/CeZrO at 1 atm and 850 °C at different gas compositions: (1) CH_4:H_2O:CO_2:O_2 = 1:0.6:0.6:0; (2) CH_4:H_2O:CO_2:O_2 = 1:0.49:0.49:0.11; (3) CH_4:H_2O:CO_2:O_2 = 1:0.38:0.38:0.22; (4) CH_4:H_2O:CO_2:O_2 = 1:0.27:0.27:0.33. (All the ratios are mol ratios; CH_4 flow rate = 25 ml/min.)

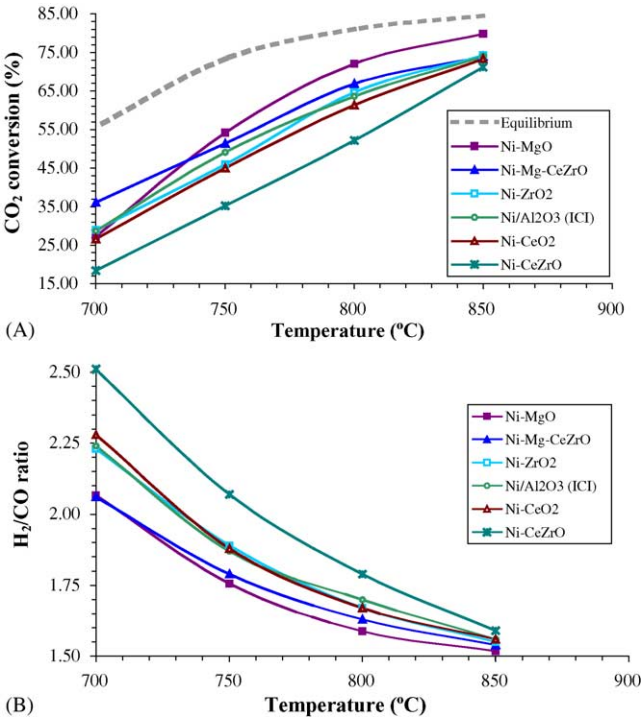

Fig. 17. (A) CO_2 conversions in the tri-reforming reaction over 100 mg supported Ni catalysts at 1 atm and feed composition of CH_4:CO_2:-H_2O:O_2 = 1:0.48:0.54:0.1 (CH_4 flow rate = 25 ml/min). (B) H_2/CO ratios in the tri-reforming reaction over 100 mg supported Ni catalysts at 1 atm and feed composition of CH_4:CO_2:H_2O:O_2 = 1:0.48:0.54:0.1 (CH_4 flow rate = 25 ml/min).

7.2. Comparison of different Ni catalysts for tri-reforming

CO_2-TPD indicates that Ni/MgO, Ni/CeZrO, and Ni/MgO/CeZrO have stronger interaction with CO_2 than Ni/Al_2O_3, Ni/CeO_2, and Ni/ZrO_2. These catalysts were then examined in tri-reforming.

Figs. 16 and 17 show the CH_4 conversion, CO_2 conversion, and H_2/CO ratio, respectively, for tri-reforming over Ni/MgO, Ni/MgO/CeZrO, Ni/Al_2O_3 (ICI catalyst), Ni/ZrO_2, Ni/CeO_2, and Ni/CeZrO. The feed for tri-reforming had the composition of CH_4:CO_2:H_2O:O_2 (mol ratio) = 1:0.48:0.54:0.1. Almost equal amounts of CO_2 and H_2O in the feed were intentionally selected for the convenience of comparing CO_2 conversions in the presence of an equal amount of H_2O in tri-reforming. The tri-reforming reactions were conducted at 700–850 °C and 1 atm at the space velocity of ca. 32,000 ml/(h g cat.) in a quartz reactor. Under all these reaction conditions, O_2 conversion is always 100%. Ni/MgO, Ni/MgO/CeZrO, Ni/ZrO_2, and Ni/Al_2O_3 (ICI catalyst) have almost the same CH_4 conversions at 800–850 °C, while Ni/CeO_2 and Ni/CeZrO have relatively lower CH_4 conversions. With the reaction temperature decreasing, CH_4 conversion over Ni/MgO declines much faster than that over other catalysts. At 700 °C, the CH_4 conversion over Ni/MgO is the lowest among all the tested catalysts. We speculate that the deactivation of Ni/MgO at lower temperatures cause the fast decline of CH_4 conversion over Ni/MgO and the deactivation is caused by the re-oxidation of Ni. This speculation is justified by the facts that NiO in the NiO/MgO catalyst is not reducible at temperature below 750 °C and no carbon formation is observed on the used Ni/MgO catalyst (see below). In addition, metal sintering may not be the reason for deactivation because all the catalytic performance tests were

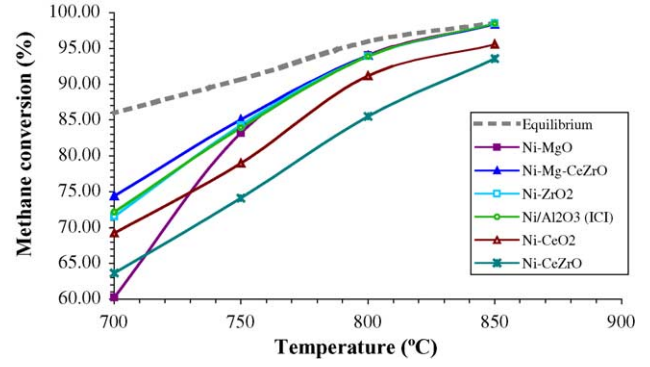

Fig. 16. CH_4 conversions in the tri-reforming reaction over 100 mg supported Ni catalysts at 1 atm and feed composition of CH_4:CO_2:-H_2O:O_2 = 1:0.48:0.54:0.1 (CH_4 flow rate = 25 ml/min).

first carried out at 850 °C. Then the reaction temperatures were gradually decreased to 700 °C.

Among all the tested catalysts, Ni/CeO_2 has the second lowest CH_4 conversion at reaction temperatures above 750 °C. The low CH_4 conversion over Ni/CeO_2 is probably related to the larger Ni particles over Ni/CeO_2 or the occurring of strong metal–support interaction (SMSI) due to the partial reduction of CeO_2 at high temperatures. Surprisingly, Ni/CeZrO has the lowest CH_4 conversion.

Although Ni/MgO, Ni/MgO/CeZrO, Ni/Al_2O_3 (ICI catalyst), and Ni/ZrO_2 have similar CH_4 conversions, their CO_2 conversions are quite different. Ni/MgO shows the highest CO_2 conversion at temperatures above 750 °C, followed by Ni/MgO/CeZrO. Ni/CeO_2 and Ni/CeZrO again show the lowest CO_2 conversion.

The H_2/CO ratio in the products depends mainly on the CO_2 and H_2O conversions in tri-reforming. If more H_2O is converted than CO_2, then the H_2/CO ratio in the product would be higher. Similarly, if less H_2O is converted than CO_2, the H_2/CO ratio would be lower. Therefore, the H_2/CO ratio is a good indicator for comparing the ability to convert CO_2 in the presence of H_2O over different catalysts. Ni/MgO gives the lowest H_2/CO ratio, followed by Ni/MgO/CeZrO. The H_2/CO ratios over Ni/CeO_2, Ni/ZrO_2, and Ni/Al_2O_3 (ICI catalyst) are similar and slightly higher than Ni/MgO/CeZrO. Ni/CeZrO gives the highest H_2/CO ratio. These results strongly suggest that Ni/MgO enhance the CO_2 conversion most in the presence of H_2O and O_2. Among all the tested catalysts, their ability to enhance the conversion of CO_2 follows the order of Ni/MgO > Ni/MgO/CeZrO > $Ni/CeO_2 \approx Ni/ZrO_2 \approx Ni/Al_2O_3$ (ICI) > Ni/CeZrO.

The different ability to convert CO_2 over different catalysts in tri-reforming is related to the properties of the catalysts. The enhancement of CO_2 conversion over Ni/MgO might be related to its enhanced CO_2 adsorption ability as evidenced by the CO_2-TPD results. However, catalysts supported on CeZrO (e.g., Ni/MgO/CeZrO and Ni/CeZrO) do not show more enhancement of CO_2 conversion than Ni/MgO even though these catalysts demonstrate more and stronger CO_2 adsorption than Ni/MgO as indicated by the large CO_2 desorption peaks at 710–717 °C.

In addition to the tests with a quartz reactor, we also conducted tri-reforming in a fixed-bed stainless steel reactor with a similar dimension. Fig. 18 shows the time-on-stream profiles for CO_2 and CH_4 conversions in the tri-reforming reaction over Ni/MgO/CeZrO catalyst at 850 °C under 1 atm with feed composition of $CH_4:CO_2:H_2O:O_2 = 1:0.475:0.475:0.1$ (CH_4 flow rate = 25 ml/min, in a stainless reactor). The catalyst was pre-reduced following a specific procedure described above, which is based on a prior study in our laboratory on the effect of pre-reduction of Ni catalysts on the reforming. It is clear that the catalyst shows a stable activity for the tri-reforming from the beginning to the end of the 5 h time-on-stream. The H_2/CO ratio also remained stable during the whole period of the time-on-stream.

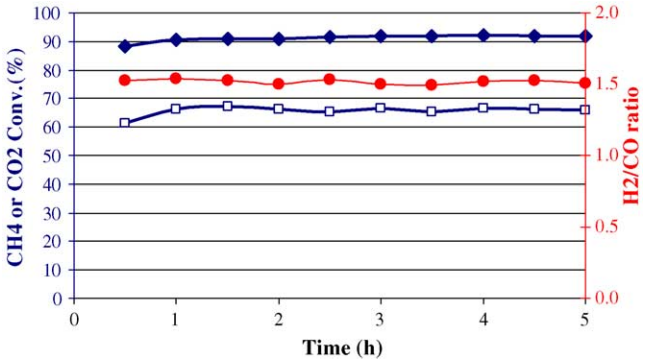

Fig. 18. Time-on-stream profiles for CO_2 and CH_4 conversions in the tri-reforming reaction over Ni/MgO/CeZrO catalyst at 850 °C under 1 atm with feed composition of $CH_4:CO_2:H_2O:O_2 = 1:0.475:0.475:0.1$ (CH_4 flow rate = 25 ml/min, in a stainless reactor).

7.3. Desired feed gas compositions for tri-reforming?

Are there more desired feed gas compositions for tri-reforming if one wishes to pursue tri-reforming with or without specific flue gas? The answer is yes in general. It usually depends on the specific product H_2/CO ratio required and the need for external heating. For the production of syngas with H_2/CO ratio of 2.0 and with high CO_2 conversion, the best feed composition would be $CH_4:CO_2:H_2O:O_2 = 1:0.3–0.4:0.6–0.8:0.1–0.2$. For the production of syngas with H_2/CO ratio of 1.5 and with high CO_2 conversion, the best feed composition would be $CH_4:CO_2:H_2O:O_2 = 1:0.4–0.5:0.4–0.5:0.1–0.2$.

As a rule of thumb, for obtaining product H_2/CO of 2, $CO_2:H_2O$ molar ratio in the feed should be close to 1:2. On the other hand, if H_2/CO of 1.5 is required, $CO_2:H_2O$ ratio in the feed should be close to 1:1. On the other hand, tri-reforming is flexible for meeting different process requirements by changing the $CH_4:CO_2:H_2O:O_2$ ratio. For example, for reducing the need for external heating, more O_2 can be incorporated in the feed gas. However, if high CO_2 conversion is desired in tri-reforming, less O_2 in feed gas is preferred.

8. Elimination of carbon formation by tri-reforming compared to CO_2 reforming

Carbon formation is an important issue in reforming of natural gas. As discussed in previous section, one advantage of tri-reforming is its potential to eliminate carbon deposition on catalysts, which is often a problem encountered in the CO_2 reforming reaction. Therefore, we conducted temperature-programmed oxidation of the used catalysts from the above tri-reforming experiments. The catalysts after the catalytic performance tests for about 6 h in tri-reforming were unloaded from the reactor and further analyzed by the carbon analyzer to check whether there is

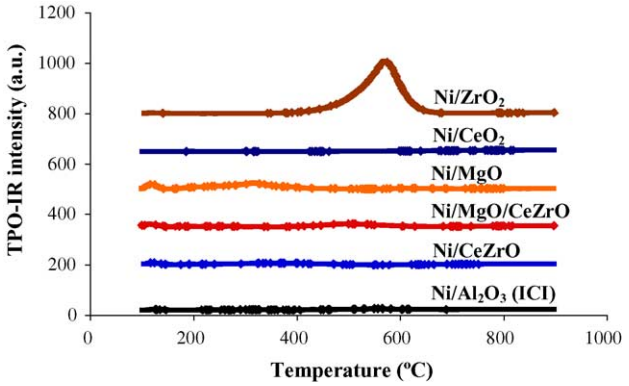

Fig. 19. Carbon analysis on the catalysts by TPO-IR after tri-reforming reaction.

carbon deposition over these used catalysts after tri-reforming.

Fig. 19 shows the results of carbon analysis over these used catalysts. No carbon formation is observed on used Ni/CeO_2, Ni/CeZrO, Ni/MgO/CeZrO, Ni/MgO, and not even on used Ni/Al_2O_3 (ICI), except for a small amount of carbon (1.34 wt.%) detected on Ni/ZrO_2. These results are consistent with the thermodynamic analysis for carbon formation shown in Fig. 4. Therefore, the advantage of tri-reforming is clearly demonstrated with respect to carbon-free processing. Tri-reforming can convert CO_2 into synthesis gas and, at the same time, eliminate or significantly carbon formation which is often a problem encountered in the CO_2 reforming reaction.

We have also tested a commercially available Haldor-Topsoe R67 Ni-based catalyst for tri-reforming in a fixed-bed flow reactor using gas mixtures that simulate the cases with flue gases from coal-fired power plants (CO_2:H_2O:-CH_4:O_2 = 1:1:1:0.1, mol ratio) and from natural gas-fired power plants (CO_2:H_2O:CH_4:O_2 = 1:2:1:0.1, mol ratio) [7,8]. For CO_2 reforming of CH_4, carbon formation is an important problem [12–15]. Temperature-programmed oxidation (TPO) results show that the used Haldor-Topsoe R67 catalyst after 300 min time-on-stream for CO_2 reforming at 850 °C and 1 atm contained 21.8 wt.% carbon [7,8]. On the other hand, the same catalyst employed in tri-reforming showed no sign of carbon formation after 300 min TOS, as the used catalyst appears to be greenish powders (versus the black powders from CO_2 reforming) [7,8]. Therefore, our results show that tri-reforming can be performed with stable operation, and no carbon formation and no appreciable deactivation of catalyst were observed under the tri-reforming conditions.

9. Kinetic study on the tri-reforming over supported Ni catalysts

The results of catalytic performance tests described above have shown that Ni catalysts supported on different supports have different ability to convert CO_2 in the presence of H_2O and O_2. However, these tests were conducted at conditions close to equilibrium conversions at 850 °C. Hence, a kinetic study was conducted to further examine the effect of supports on the catalytic performance, especially the conversion of CO_2 in the presence of H_2O and O_2 over different catalysts.

For the kinetic study, the CH_4 conversion and CO_2 conversion were kept in the range of 10–20% in order to obtain close to differential conditions. These conversions were not further reduced to less than 10% considering the relative low sensitivity of CO_2 detection by TCD detector when Ar is used as a carrier gas. The kinetic study was carried out at 850 °C and 1 atm at conditions free of significant internal and external diffusion effects. These conditions were checked by using the Weisz criterion [44] as well as the experimental Boudart test on diffusion effects [45] over different volumes and different particle sizes of catalysts [10].

The kinetic study was based on the power rate law as shown in Eq. (1′):

$$r(\mathrm{i}) = A \exp\left(\frac{-E_{\mathrm{app,i}}}{RT}\right)(P_{\mathrm{CO_2}})^{\alpha,\mathrm{i}}(P_{\mathrm{H_2O}})^{\beta,\mathrm{i}} \qquad (1')$$

where i is CH_4 or CO_2, r(i) the CH_4 or CO_2 conversion rate, A the pre-exponential factor, (α,i), (β,i) the reaction orders, and $E_{\mathrm{app,i}}$ is the apparent activation energy with respect to CH_4 or CO_2 conversion.

It should be noted that Eq. (1′) could also include the items containing the partial pressures of CH_4 and O_2. In this study, however, we chose to keep the partial pressures of CH_4 and O_2 constant and focus on identifying the difference of CO_2 conversion over different catalysts. Therefore, the items containing the partial pressures of CH_4 and O_2 can be regarded as constant and combined with other constants in Eq. (1′) (e.g., A).

By measuring the CH_4 or CO_2 conversion rates at different temperatures and at different CO_2 or H_2O partial pressures (Argon was used as a balance gas in order to maintain the total gas flow rate constant), the apparent activation energy ($E_{\mathrm{app,i}}$) and the reaction order (α or β) with respect to CO_2 or H_2O partial pressures could be estimated.

Figs. 20–23 show the plots of ln(r(CH_4)) or ln(r(CO_2)) versus ln(P_{CO_2}) or ln(P_{H_2O}) and Figs. 24 and 25 show the plots of ln(r(CH_4)) or ln(r(CO_2)) versus 1/T over Ni/Al_2O_3 (ICI catalyst), Ni/MgO/CeZrO, and Ni/MgO. The estimated reaction orders (α or β) and apparent activation energies ($E_{\mathrm{app,i}}$) derived from these plots are listed in Table 4.

It is interesting to notice from Figs. 20 and 21 and Table 4 that P_{CO_2} has different effects on CH_4 conversion rate over Ni/Al_2O_3 (ICI catalyst), Ni/MgO/CeZrO, and Ni/MgO. The CH_4 conversion rate has a slight increase over Ni/Al_2O_3 (corresponding to the reaction order of 0.79 ± 0.40) with the increase of P_{CO_2} and is almost unchanged over Ni/MgO/CeZrO (corresponding to the reaction order of 0.00 ± 0.17). Over Ni/MgO, however, the CH_4 conversion rate decreases

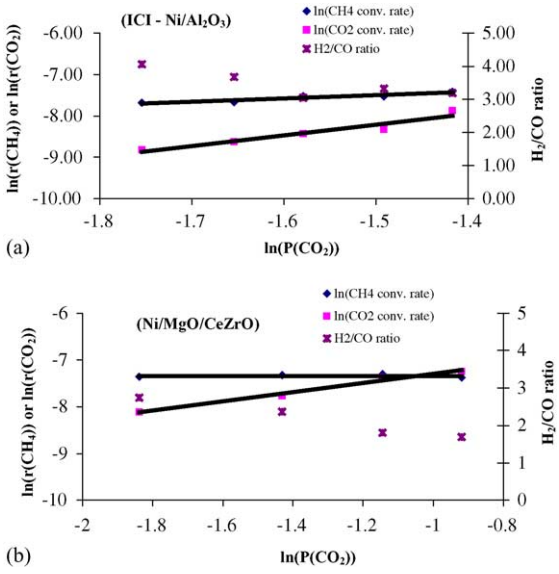

Fig. 20. CO_2 partial pressure effect on CH_4 and CO_2 conversion rates (unit: mol/s g cat.) and H_2/CO ratio at 850 °C and 1 atm over (a) Ni/Al_2O_3 (ICI) 12.8 mg, CH_4:(CO_2 + Ar):H_2O:O_2 = 1:0.81:0.54:0.02, CH_4 = 75 ml/min; (b) Ni/MgO/CeZrO 4.8 mg, CH_4:(CO_2 + Ar):H_2O:O_2 = 1:1.48:0.54:0.02, CH_4 = 25 ml/min.

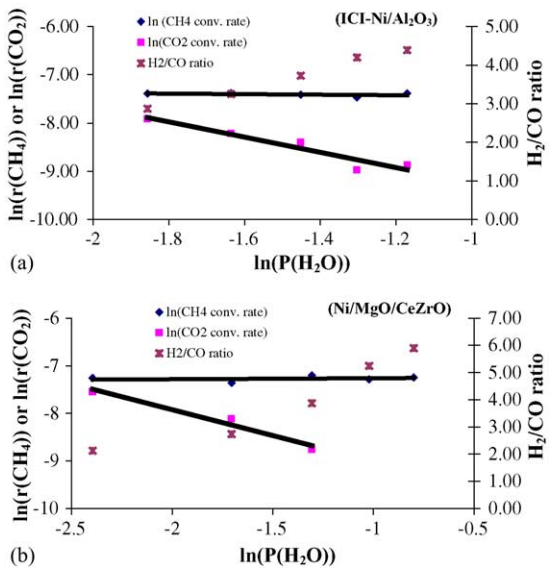

Fig. 22. H_2O partial pressure effect on CH_4 and CO_2 conversion rates (unit: mol/s g cat.) and H_2/CO ratio at 850 °C and 1 atm over (a) Ni/Al_2O_3 (ICI) 12.8 mg, CH_4:CO_2:(H_2O + Ar):O_2 = 1:0.48:0.87:0.02, CH_4 = 75 ml/min; (b) Ni/MgO/CeZrO 4.8 mg, CH_4:CO_2:(H_2O + Ar):O_2 = 1:0.48:1.54:0.02, CH_4 = 25 ml/min.

with the increase of P_{CO_2}, resulting in a negative reaction order (-0.87 ± 0.17) with respect to P_{CO_2}.

These results show the different kinetics of CH_4 conversion by CO_2 in the presence of H_2O and O_2 over different catalysts. To understand what causes these differences, further studies on detailed reaction mechanisms are necessary. At the present stage, it is likely that the different extent of interaction between CO_2 and catalysts could be responsible for these differences. To illustrate how the interaction between CO_2 and a catalyst could change the reaction order of CH_4 conversion rate, we can use CO_2 reforming of methane as an example based on a simplified Langmuir–Hinshelwood (L–H) mechanism:

$$CH_4 + * = CH_4^* \qquad K_{CH_4} = \frac{[CH_4^*]}{P_{CH_4}[*]} \tag{2'}$$

$$CO_2 + * = CO_2^* \qquad K_{CO_2} = \frac{[CO_2^*]}{P_{CO_2}[*]} \tag{3'}$$

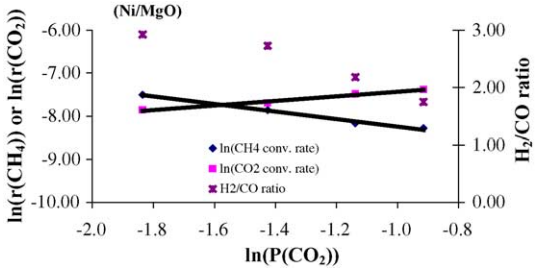

Fig. 21. CO_2 partial pressure effect on CH_4 and CO_2 conversion rates (unit: mol/s g cat.) and H_2/CO ratio at 850 °C and 1 atm over Ni/MgO catalyst, 5.1 mg, CH_4:(CO_2 + Ar):H_2O:O_2:H_2 = 1:1.28:0.54:0.02:0.2, CH_4 = 25 ml/min.

$$CH_4^* + CO_2^* \rightarrow 2CO + 2H_2 + 2^* \tag{4'}$$

rate determining step : k (rate constant)

Therefore, CH_4 conversion rate could be expressed as:

$$r(CH_4) = \frac{kK_{CH_4}K_{CO_2}P_{CH_4}P_{CO_2}}{[1 + K_{CH_4}P_{CH_4} + K_{CO_2}P_{CO_2}]^2} \tag{5'}$$

Depending on the relative size of $K_{CH_4}P_{CH_4}$, $K_{CO_2}P_{CO_2}$, and 1 in the denominator of Eq. (5′), the reaction order of CH_4 with respect to CO_2 could change from 1 when $K_{CO_2}P_{CO_2} \ll$ (1 and $K_{CH_4}P_{CH_4}$) to -1 when $K_{CO_2}P_{CO_2} \gg$ ($K_{CH_4}P_{CH_4}$ and 1). K_{CO_2} is closely related to the interaction of CO_2 with catalysts. When CO_2 has strong interaction with a catalyst, K_{CO_2} may be larger than K_{CH_4} and $K_{CO_2}P_{CO_2}$ become dominant in the denominator of Eq. (5′). In another word, adsorbed CO_2 species may become the most abundant reaction intermediate on the catalyst. With the increase of CO_2 partial pressure, more sites are occupied by adsorbed CO_2 species and less sites are available for CH_4 adsorption.

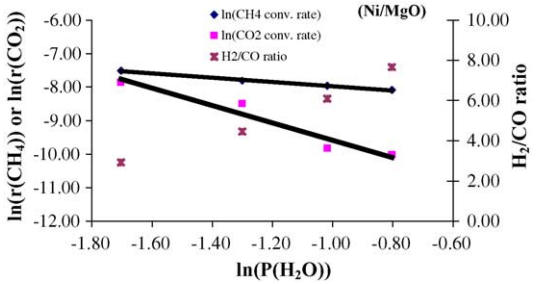

Fig. 23. H_2O partial pressure effect on CH_4 and CO_2 conversion rates (unit: mol/s g cat.) and H_2/CO ratio at 850 °C and 1 atm over Ni/MgO, 5.1 mg, CH_4:CO_2:(H_2O + Ar):O_2:H_2 = 1:0.48:1.34:0.02:0.2, CH_4 = 25 ml/min.

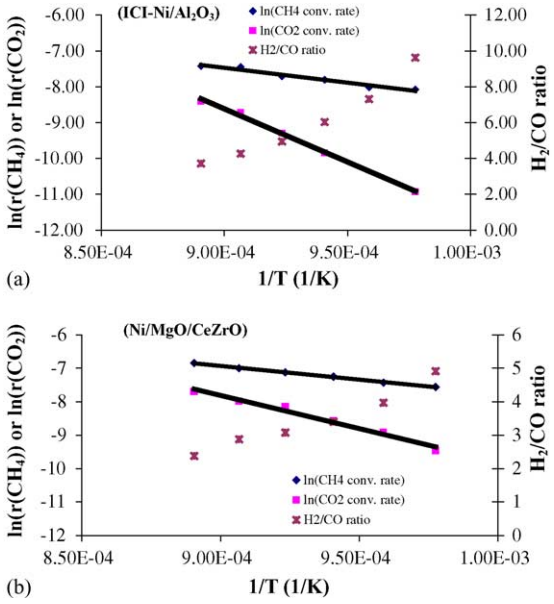

Fig. 24. Plots of ln(CH_4 conversion rate (mol/s g cat.)), ln(CO_2 conversion rate (mol/s g cat.)), and H_2/CO ratio vs. $1/T$ over (a) Ni/Al_2O_3 (ICI) 12.8 mg, at constant feed composition of CH_4:CO_2:H_2O:O_2:Ar = 1:0.48:0.54:0.02:0.33, CH_4 = 75 ml/min; (b) Ni/MgO/CeZrO 4.8 mg, at constant feed composition of CH_4:CO_2:H_2O:O_2:Ar = 1:0.48:0.54:0.02:1, CH_4 = 25 ml/min.

As a result, CH_4 conversion rate decreases with increasing P_{CO_2} and shows the negative reaction order with respect to P_{CO_2}. Similarly, when CO_2 has a weak interaction with a catalyst, K_{CO_2} may be smaller than K_{CH_4}. CH_4 conversion rate can have a positive reaction order with respect to P_{CO_2}. This explains why the reaction order of CH_4 conversion with respect to P_{CO_2} is positive over Ni/Al_2O_3 and negative over Ni/MgO. In fact, our CO_2-TPD results have shown that CO_2 adsorption is stronger on Ni/MgO than on Ni/Al_2O_3. Horicuchi et al. [46] also reported that the heat of adsorption of CO_2 on γ-Al_2O_3 is smaller than that on MgO modified γ-Al_2O_3. Over γ-Al_2O_3, the heat of adsorption of CO_2 is estimated to be 90 kJ/mol at zero surface coverage, while the heat of adsorption over MgO modified γ-Al_2O_3 is about 130 kJ/mol.

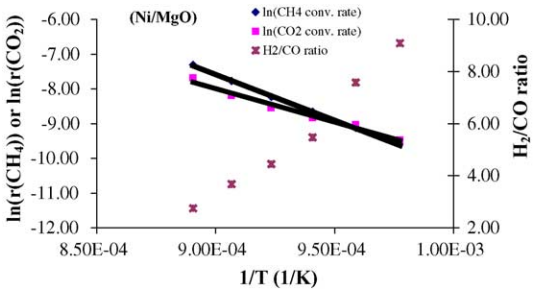

Fig. 25. Plots of ln(CH_4 conversion rate (mol/s g cat.)), ln(CO_2 conversion rate (mol/s g cat.)), and H_2/CO ratio vs. $1/T$ over Ni/MgO catalyst, 5.1 mg, at constant feed composition of CH_4:CO_2:H_2O:O_2:H_2:Ar = 1:0.48:0.54:0.02:0.2:0.8, CH_4 = 25 ml/min.

Table 4
Results of kinetic study on tri-reforming

850 °C	Catalysts		
	Ni/Al_2O_3 (ICI)	Ni/MgO/CeZrO	Ni/MgO
P_{CO_2} effect			
α, CH_4	0.79 ± 0.40	0.00 ± 0.17	-0.87 ± 0.17
α, CO_2	1.90 ± 0.99	0.98 ± 0.25	0.53 ± 0.13
P_{H_2O} effect			
β, CH_4	-0.06 ± 0.18	0.03 ± 0.16	-0.64 ± 0.09
β, CO_2	-1.57 ± 0.66	-1.08 ± 0.37	-2.59 ± 1.09
Apparent activation energy (kJ/mol)			
E_{app}, CH_4	69.1 ± 20.2	67.4 ± 3.4	219.6 ± 10.5
E_{app}, CO_2	247.0 ± 24.4	165.7 ± 26.4	160.1 ± 32.2

Kinetic data are reported as $r(\mathrm{i}) = A \exp(-E_{app,i}/RT)\ (P_{CO_2})^{\alpha,i}\ (P_{H_2O})^{\beta,i}$, i = CH_4 or CO_2.

Different from Ni/MgO, the reaction order of CH_4 conversion with respect to P_{CO_2} over Ni/MgO/CeZrO is close to zero, indicating that the CH_4 conversion rate almost does not change with P_{CO_2} even thought it is found that Ni/MgO/CeZrO has even more and stronger interaction with CO_2 than Ni/MgO, as evidenced by their CO_2-TPD profiles. This implies that the sites for strong CO_2 adsorption over Ni/MgO/CeZrO are probably not the same as or close enough to those for CH_4 adsorption and conversion. Ni itself is believed to be able to activate CH_4 as indicated by Rostrup-Nielsen [47], while supports such as MgO are capable to adsorb CO_2. Hence, the interfaces between Ni and supports are very important locations where most of the reaction takes place [48–51]. It has been shown from our XRD results that NiO and MgO form a solid solution in NiO/MgO. The formation of NiO/MgO solid solution results in the difficult reduction of NiO, yet it provides highly dispersed Ni particles once NiO is reduced. This provides more interface between Ni and MgO. On the other hand, although part of the NiO also forms a solid solution with the small amount of MgO in Ni/MgO/CeZrO, some isolated NiO is still observed, as indicated by the lower-temperature reduction peaks in the Ni/MgO/CeZrO TPR profile. These Ni particles reduced at a lower temperature tend to have larger size and have less interface between themselves and the support. Similarly, over Ni/CeZrO without the promotion of MgO, almost all the Ni can be reduced below 850 °C and have an average particle size of 16.4 nm. Even though Ni/CeZrO is capable of CO_2 adsorption, the adsorbed CO_2 is found not to be useful probably because the sites for CO_2 adsorption on Ni/CeZrO are different from those for CH_4 adsorption. This may explain why Ni/CeZrO without MgO promotion has the lowest CO_2 conversion and CH_4 conversion.

The reaction orders for CO_2 conversion with respect to P_{CO_2} are also found to decrease in the order of Ni/Al_2O_3 (1.90 ± 0.99) < Ni/MgO/CeZrO (0.98 ± 0.25) < Ni/MgO (0.53 ± 0.13), consistent with their ability for CH_4 conversion. Considering that P_{CO_2} is always less than 1, a low reaction order with respect to P_{CO_2} always results in a high

CO_2 conversion rate if other parameters in Eq. (1′) are the same.

The reaction orders with respect to P_{H_2O} for CH_4 conversion over Ni/Al_2O_3 and Ni/MgO/CeZrO are both close to zero. A negative reaction order (-0.64 ± 0.09) is again observed over Ni/MgO. However, the reaction order with respect to P_{H_2O} is less negative than the reaction order with respect to P_{CO_2}. Based on the previous discussion on reaction orders, CO_2 likely interact more strongly with Ni/MgO than H_2O. This result partially supports our hypothesis for designing a catalyst to enhance CO_2 conversion in tri-reforming.

The reaction orders for CO_2 conversion with respect to P_{H_2O} are all negative over Ni/Al_2O_3, Ni/MgO/CeZrO, and Ni/MgO, indicating that both H_2O and CO_2 are capable of reacting with CH_4 and they compete with each other to react with CH_4 to form CO and H_2. With the increase of P_{H_2O}, H_2O may become the dominant component to react with CH_4. As a result, CO_2 conversion rate decreases with the increase of P_{H_2O}. In addition, the existence of water gas shift reaction in the tri-reforming process may also play a role in decreasing the CO_2 conversion rate with the increase of P_{H_2O}.

The apparent activation energy for CH_4 conversion is found to be similar over Ni/Al_2O_3 (69.1 ± 20.2 kJ/mol) and Ni/MgO/CeZrO (67.4 ± 3.4 kJ/mol). The apparent activation energy over Ni/MgO (219.6 ± 10.5 kJ/mol) is probably overestimated due to the deactivation of Ni/MgO when reaction temperature decreases from 850 to 750 °C. As explained in the catalytic performance tests, the deactivation is likely caused by the loss of active sites due to the re-oxidation of Ni at lower temperatures in the presence of H_2O, CO_2, and O_2. Bradford [44] also observed the easy deactivation of Ni/MgO in the CO_2 reforming reaction. This deactivation was found not to result from carbon formation, but to be due to the difficulty of maintaining the active sites over Ni/MgO. At lower temperatures or at high H_2O or CO_2 partial pressures, reduced Ni may be reoxidized to its oxide state, resulting in the loss of active sites and deactivation.

In addition, the high apparent activation energy over Ni/MgO could also be attributed to the strong interaction between Ni and MgO. Ruckenstein and Hu [30] reported that the activation of CO becomes less over Ni/MgO. CO is activated on Ni when there is electron donation from Ni particles to the antibonding orbitals of the CO molecules. When Ni has strong interaction with MgO, the electron donor ability of Ni in the Ni/MgO catalyst decreases, and consequently, the activation of CO becomes less. The same explanation may also apply to the activation of CH_4 on Ni/MgO. Horicuchi et al. [46] observed that the ability for CH_4 dehydrogenation is decreased when basic metal oxides are added onto Ni/Al_2O_3.

Over Ni/Al_2O_3, the apparent activation energy for CO_2 conversion is 247.0 ± 24.4 kJ/mol, which is much higher than those over Ni/MgO/CeZrO (165.7 ± 26.4 kJ/mol) and Ni/MgO (160.1 ± 32.2 kJ/mol). Considering the loss of active sites at lower temperatures over Ni/MgO, the apparent activation energy of 160.1 ± 32.2 kJ/mol may be overestimated for Ni/MgO as well. Therefore, the apparent activation energy for CO_2 conversion is consistent with the ability of CO_2 conversion over Ni/Al_2O_3, Ni/MgO/CeZrO, and Ni/MgO. These results again partially support the hypothesis of designing a catalyst for enhancing CO_2 conversion in the presence of H_2O and O_2.

The H_2/CO ratio in the products is related to the conversion of H_2O, CO_2, and O_2. During the kinetic study of the partial pressure effect of CO_2 and H_2O, it is found that H_2/CO ratio declines with the increase of CO_2 partial pressures and increases with the increase of partial pressure of H_2O over Ni/Al_2O_3, Ni/MgO/CeZrO, and Ni/MgO. As described previously, the H_2/CO ratio in the products decreases when more CO_2 participates in CH_4 conversion. Similarly, when more H_2O participates in CH_4 conversion, the H_2/CO ratio increases. The H_2/CO ratio is also found to increase with the decrease of reaction temperatures, which is similar to the observation in the catalyst performance tests and is consistent with the trend predicted by the thermodynamic analysis. One explanation for the higher H_2/CO ratios at lower reaction temperatures is the water gas shift reaction, which is favored at low temperatures. Consequently, H_2O conversion should become more dominant compared with CO_2 conversion as reaction temperatures decrease.

10. Does tri-reforming consume more energy than CO_2 reforming or steam reforming?

A comparative energy analysis by calculation indicated that tri-reforming is more desired for producing syngas with H_2/CO ratios of 1.5–2.0 compared to CO_2 reforming and steam reforming of methane, in terms of less amount of energy required and less net amount of CO_2 emitted in the whole process for producing synthesis gas with H_2/CO ratio of 2.0 [8]. We did a comparative analysis of different processes with respect to the relative energy requirements for producing syngas with desired H_2/CO ratio of 2.0 and the amount of CO_2 produced per unit syngas ($CO + 2H_2$). Since steam reforming process has been well established in gas industries for several decades, and CO_2 reforming is being studied worldwide, these two processes are representative ones for comparison with the proposed tri-reforming. In our simplified analysis by calculation, the amount of CO_2 produced is estimated by considering: (1) the CO_2 as either product or product of reaction processes, and (2) the CO_2 equivalent to the energy requirement, which is provided by combustion of natural gas (CH_4) that produces CO_2. Total heat required for heat-up of reacting components to the reaction temperature is similar for all the three processes, except for inert gas. Current flue gases from power plants contain high concentrations of inert N_2, hence we also considered heat-up cost for the inert N_2 and the equivalent

CO_2 production due to heating. [It is likely that the use of oxygen or oxygen-enriched air is a future direction in combustion and even gasification, so the future flue gas is likely to contain much less inert gas.]

In CO_2 reforming, 0.75 mol of CH_4 and 0.75 mol of CO_2 produce 1.5 mol of H_2 and 1.5 mol of CO stoichiometrically. To obtain syngas with H_2/CO ratio of 2, 0.5 mol of CO needs to be converted and extra 0.5 mol of H_2 should be produced through water gas shift reaction. Energy is involved in all the process described above. The reaction between 0.75 mol of CH_4 and 0.75 mol of CO_2 requires 185 kJ of energy ($=0.75 \times \Delta H^\circ = 0.75 \times 247 = 185$ kJ). Another energy-demanding process is to obtain pure CO_2 for CO_2 reforming reaction. If considering that pure CO_2 is derived from a process based on monoethanolamine absorption which is indeed widely used in industries, it requires 120 kJ of energy ($=0.75 \times 160$ kJ/mol CO_2 separated from flue gas) to obtain 0.75 mol of pure CO_2. Although water gas shift reaction is slightly exothermic, this reaction heat is not taken into account since this heat is mostly not usable in CO_2 reforming reaction. Provided that all the required energy is from methane combustion, which provides 880 kJ energy/mol of methane, and thermal efficiency is 80% for external heating, then the amount of methane used through combustion to provide the required energy is 0.43 mol ([120 + 185]/0.8/880 = 0.43 mol). As far as the net CO_2 emission is concerned after all these processes, CO_2 reforming itself converts 0.75 mol of CO_2, yet water gas shift reaction produces 0.5 mol of CO_2. Methane combustion produces another 0.43 mol of CO_2. Therefore, the net CO_2 emission is 0.18 mol ($-0.75 + 0.5 + 0.43 =$ 0.18 mol) per unit of syngas (CO + $2H_2$) with desired H_2/CO ratio.

Steam reforming that is widely used in gas industries produces H_2/CO ratio that is too high (≥ 3) for either Fischer–Tropsch or methanol synthesis. When syngas with H_2/CO ratios of 2 or lower is required, CO_2 is imported. For example, the CALCOR process from Caloric, GmbH, is a steam methane reformer using a specially developed staged catalyst and an amine acid gas removal system, where CO_2 recovered from the amine system is added to the reformer [2]. The SPARG process from Haldor-Topsoe is similar to a steam reformer except that sulfur is added to partially poison the catalyst, which allows the use of CO_2 under steam reforming conditions [2]. Such factor is also considered here. In the case of steam reforming, to produce syngas with 2 mol of hydrogen and 1 mol of CO, both steam reforming and reverse water gas shift reaction are required. 0.75 mol of CH_4 first react with 0.75 mol of steam, which gives 0.75 mol of CO and 2.25 mol of hydrogen. Then 0.25 mol of CO_2 is used to convert 0.25 mol of hydrogen into H_2O and produce extra 0.25 mol of CO. Therefore, the net amounts of hydrogen and CO produced are 2 and 1 mol, respectively. For the energy required, 0.75 mol of CH_4 reacting with 0.75 mol of H_2O needs 154.5 kJ of energy input. To obtain 0.25 mol of pure CO_2 used in reverse water gas shift reaction, 40 kJ energy is required ($=0.25 \times 160$ kJ/mol CO_2). And reverse water gas shift reaction itself is slightly endothermic, which requires 10.2 kJ of energy ($=0.24 \times 40.8$ kJ/mol). If still assuming the energy is provided by methane combustion and thermal efficiency is 80%, then the amount of methane used for combustion is 0.29 mol ([154.4 + 40 + 10.2]/0.8/880 = 0.29 mol). The net CO_2 emission would be 0.04 mol since methane combustion produces 0.29 mol of CO_2 and reverse water gas shift reaction consumes 0.25 mol of CO_2.

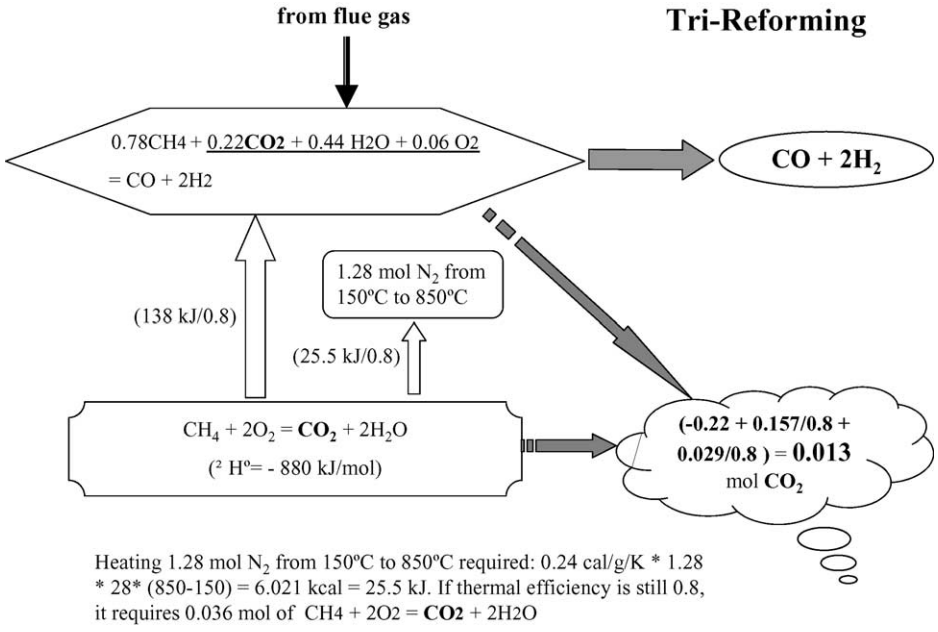

Fig. 26. Schematic showing the theoretical amount of CO_2 that may be produced per unit amount of desired syngas (CO + $2H_2$) from tri-reforming using power-plant flue gas at 850 °C.

In tri-reforming, syngas with H_2/CO ratio of 2.0 can be produced in one single step (Figs. 1 and 26). A typical flue gas from natural gas-fired power plants may contain 11% CO_2, 22% H_2O, 3% O_2, and 64% N_2. As illustrated in Fig. 26, tri-reforming of 0.78 mol of CH_4 using 2 mol of this type of flue gas could directly produce 1 mol of CO and 2 mol of H_2, which requires 138 kJ of energy (calculated from the sum of steam reforming, CO_2 reforming, and partial oxidation). Besides this energy requirement, the energy (about 25.5 kJ) for heating N_2 (1.28 mol) in flue gas from 150 °C to a typical reaction temperature (e.g., 850 °C) is also considered here. Since tri-reforming does not need pure CO_2 pre-separation, the energy needed to obtain pure CO_2 as encountered in CO_2 reforming process is not necessary. Therefore the total energy requirement is 163.5 kJ and the amount of methane for combustion is 0.233 mol (163.5/0.8/880 = 0.233 mol) if based on the same assumptions as described above. The net CO_2 emission is 0.013 mol since tri-reforming eliminates 0.22 mol of CO_2 and methane combustion produces 0.233 mol of CO_2.

It can be seen from the above comparison that, in terms of CO_2 produced based on relative energy requirements, tri-reforming process generates considerably less CO_2 per unit amount of desired syngas (CO + $2H_2$), than the industrial steam reforming process and the well-known CO_2 reforming process. In other words, the above analysis indicates that tri-reforming produces the least CO_2 among the three processes for syngas production. In terms of CO_2 utilization, the comparisons on energy requirement and net CO_2 emissions show that compared to CO_2 reforming, tri-reforming using flue gas is less energy intensive and more efficient when syngas with H_2/CO of 1.5–2 is desired.

11. Independent studies on tri-reforming and its potential applications

Although the tri-reforming process concept was proposed from our laboratory only 4 years ago with the first conference paper in 1999 [7–10], the term tri-reforming has been adopted in several recent reports by other research groups [52–55] and also appeared in a recent review [56]. The feasibility of tri-reforming reactions has been experimentally demonstrated in independent studies in other industrial and academic laboratories [52–55].

The tri-reforming process could be applied, in principle, to the production of industrially useful syngas (for synthesis of methanol and dimethyl ether, for Fischer–Tropsch synthesis, and for high-temperature fuel cells, etc.) by reforming of natural gas using gas mixtures (containing CO_2, H_2O, and O_2) as co-feeds. Such mixtures include, but not limited to, the flue gas from either natural gas-based electric power plant or coal-based electric power plants or the flue gas from partial oxidation units in chemical manufacturing facilities. It was recently proposed that tri-reforming could also be applied for converting low-quality CO_2-rich natural gas into industrially useful syngas [57].

12. Conclusions

Catalytic tri-reforming of methane can be achieved successfully with high CH_4 conversion ($\geq$97%) and high CO_2 conversion (around 80%) for producing syngas with desired H_2/CO ratios of 1.5–2.0 over supported nickel catalysts at 800–850 °C under atmospheric pressure without the problem of carbon formation on the catalyst. Catalysts play an important role on tri-reforming conversions and selectivity. Gas phase reaction of tri-reforming without catalyst is negligible at temperature as high as 850 °C. Carbon analysis on all the used Ni catalysts after the tri-reforming reactions has confirmed that carbon formation over catalysts is indeed significantly reduced or even eliminated in the tri-reforming system.

The CO_2 and CH_4 conversion as well as H_2/CO ratios of the products from tri-reforming also depend on the type and nature of catalysts (formulation, preparation, pre-treatment). An important observation is that CO_2 conversion can be maximized by tailoring catalyst composition and preparation method. In other words, certain catalysts with proper feature can give much higher CO_2 conversion than other catalysts under the same reaction conditions with the same reactants feed.

Among all the catalysts tested for tri-reforming, their ability to enhance the conversion of CO_2 follows the order of Ni/MgO > Ni/MgO/CeZrO > Ni/CeO_2 ≈ Ni/ZrO_2 ≈ Ni/Al_2O_3 (ICI) > Ni/CeZrO. The different ability to convert CO_2 over different catalysts in tri-reforming is related to the properties of the catalysts. The higher CO_2 conversion over Ni/MgO and Ni/MgO/CeZrO in tri-reforming may be related to the stronger interaction of CO_2 with MgO and more interface between Ni and MgO resulting from the formation of NiO/MgO solid solution.

Results of catalytic performance tests over Ni/MgO/CeZrO catalysts at 850 °C and 1 atm at different feed compositions confirm the predictions based on the thermodynamic analysis for equilibrium conversions in tri-reforming of methane.

The kinetic study indicates that the reaction orders of CH_4 conversion and CO_2 conversion rates with respect to partial pressures of CO_2 and H_2O are different over Ni/MgO, Ni/MgO/CeZrO, and Ni/Al_2O_3. The negative reaction order of CH_4 conversion rate with respect to P_{CO_2} is observed over Ni/MgO while the reaction order on Ni/MgO/CeZrO is close to zero. These results indicate that CO_2 has a strong adsorption on Ni/MgO and CO_2 adsorption sites on Ni/MgO may be the same or close to the sites for CH_4 reforming due to the formation of extensive interface between Ni and MgO, while, over Ni/MgO/CeZrO, the sites for strong CO_2 adsorption and the sites for CH_4 adsorption and CH_4 reforming may be different and isolated. Therefore, the

strongly adsorbed CO_2 on Ni/MgO/CeZrO or Ni/CeZrO may not be useful in enhancing the CO_2 conversion.

The lowest apparent activation energy for CO_2 conversion over Ni/MgO during the tri-reforming process indicates that CO_2 is relatively easier to activate over Ni/MgO than over Ni/Al_2O_3 catalyst.

Acknowledgements

The authors are grateful to the US Department of Energy, National Energy Technology Laboratory for supporting this work (UCR Innovative Concepts Program), to Prof. H.H. Schobert and Prof. A.W. Scaroni of PSU for their encouragement of CS's research on CO_2 conversion, to Prof. M.A. Vannice and Prof. L. Radovic for helpful discussions on reaction kinetics, to Mr. B. Miller and Dr. S. Pisupati of PSU for helpful discussions on power plant flue gas, and to Haldor-Topsoe and ICI for the commercial catalyst samples. CS thanks Dr. J. Armor of Air Products and Chemicals Inc. for helpful discussions on CO_2 reforming and Dr. J. Stringer of Electric Power Research Institute for helpful discussions on power plants operation.

References

[1] CO_2 Conversion and Utilization,C. Song, A.M. Gaffney, K. Fujimoto (Eds.), ACS Symp. Ser.American Chemical Society, Washington, DC, 2002.
[2] (a) M.M. Halmann, M. Steinberg, Greenhouse Gas Carbon Dioxide Mitigation: Science and Technology, Lewis Publishers, Boca Raton, FL, 1999;
(b) H. Gunardson, Industrial Gases in Petrochemical Processing, Marcel Dekker, New York, 1998.
[3] M.M. Maroto-Valer, C. Song, Y. Soong (Eds.), Environmental Challenges and Greenhouse Gas Control for Fossil Fuel Utilization in the 21st Century, Kluwer Academic/Plenum Publishers, New York, 2002
[4] DOE/OS-FE, Carbon Sequestration, State of the Science, Office of Science and Office of Fossil Energy, US DOE, 1999.
[5] T. Weimer, K. Schaber, M. Specht, A. Bandi, Am. Chem. Soc. Div. Fuel Chem. Prepr. 41 (4) (1996) 1337.
[6] DOE/FE, Capturing Carbon Dioxide, Office of Fossil Energy, US DOE, 1999.
[7] (a) C. Song, Chem. Innovation (formerly Chemtech. ACS) 31 (2001) 21;
(b) C. Song, in: Proceedings of the 16th Annual International Pittsburgh Coal Conference, University of Pittsburgh, Pittsburgh, PA, October 1999, pp. 11–15 (Paper no. 16-5);
(c) C. Song, S.T. Srimat, W. Pan, L. Sun, Am. Chem. Soc. Div. Fuel Chem. Prep. 46 (1) (2001) 101;
(d) W. Pan, J. Zheng, C. Song, Am. Chem. Soc. Div. Fuel Chem. Prep. 47 (1) (2002) 262.
[8] C. Song, W. Pan, S.T. Srimat, in: M.M. Maroto-Valer, C. Song, Y. Soong (Eds.), Environmental Challenges and Greenhouse Gas Control for Fossil Fuel Utilization in the 21st Century, Kluwer Academic/Plenum Publishers, New York, 2002, p. 247(Chapter 18).
[9] C. Song, Am. Chem. Soc. Symp. Ser. 809 (2002) 2.
[10] W. Pan, Tri-reforming and combined reforming of methane for producing syngas with desired H_2/CO ratios, Ph.D. thesis, Pennsylvania State University, 2002.
[11] W. Pan, C. Song, Am. Chem. Soc. Symp. Ser. 809 (2002) 316.
[12] C. Song, S.T. Srimat, S. Murata, W. Pan, L. Sun, A.W. Scaroni, J.N. Armor, Am. Chem. Soc. Symp. Ser. 809 (2002) 258.
[13] S.T. Srimat, C. Song, Am. Chem. Soc. Symp. Ser. 809 (2002) 289.
[14] A.M. O'Connor, J.R.H. Ross, Catal. Today 46 (2–3) (1998) 20.
[15] E. Ruckenstein, Y.H. Hu, Ind. Eng. Chem. Res. 37 (5) (1998) 1744.
[16] P.D.F. Vernon, M.L.H. Green, A.K. Cheetham, A.T. Ashcrof, Catal. Today 13 (2–3) (1992) 417.
[17] V.R. Choudhary, A.M. Rajput, B. Prabhakar, Catal. Lett. 32 (3–4) (1995) 391.
[18] V.R. Choudhary, A.S. Mamman, J. Chem. Technol. Biotechnol. 73 (4) (1998) 345.
[19] T. Inui, K. Saigo, Y. Fujii, K. Fujioka, Catal. Today 26 (3–4) (1995) 295.
[20] V.R. Choudhary, A.M. Rajput, B. Prabhakar, Angew. Chem. Int. Ed. Engl. 33 (20) (1994) 2104.
[21] V.R. Choudhary, A.M. Rajput, Ind. Eng. Chem. Res. 35 (1996) 3934.
[22] V.R. Choudhary, B.S. Uphade, A.S. Mamman, Appl. Catal., A: Gen. 168 (1998) 33.
[23] M.E.S. Hegarty, A.M. O'Connor, J.R.H. Ross, Catal. Today 42 (3) (1998) 225.
[24] S. Rossigonol, Y. Madier, D. Duprez, Catal. Today 50 (1999) 261.
[25] M.F. Mark, F. Mark, W.F. Maier, Chem. Eng. Technol. 20 (6) (1997) 361.
[26] V.C.H. Kroll, H.M. Swaan, S. Lacombe, C. Mirodatos, J. Catal. 164 (2) (1997) 387.
[27] J.R. Rostrup-Nielsen, J.H. Bak Hansen, J. Catal. 144 (1993) 38.
[28] K. Tomishige, Y. Chen, X. Li, K. Yokoyama, Y. Sone, O. Yamazaki, K. Fujimoto, Advances in chemical conversions for mitigating carbon dioxide, Stud. Surf. Sci. Catal. 114 (1998) 375.
[29] J. Nakamura, K. Aikawa, K. Sato, T. Uchijima, Catal. Lett. 25 (3–4) (1994) 265.
[30] E. Ruckenstein, Y.H. Hu, Appl. Catal. A 133 (1) (1995) 149.
[31] Y.H. Hu, E. Ruckenstein, Catal. Lett. 43 (1–2) (1997) 71.
[32] H.S. Roh, K.W. Jun, W.S. Dong, S.E. Park, Y.S. Baek, Catal. Lett. 74 (1–2) (2001) 31.
[33] O. Yamazaki, K. Tomishige, K. Fujimoto, Appl. Catal. A 136 (1) (1996) 49.
[34] E. Ruckenstein, Y.H. Hu, Ind. Eng. Chem. Res. 37 (5) (1998) 1744.
[35] A. Parmaliana, F. Arena, F. Frusteri, S. Coluccia, L. Marchese, G. Martra, A.L. Chuvilin, J. Catal. 141 (1) (1993) 34.
[36] M.C.J. Bradford, M.A. Vannice, Catal. Rev.-Sci. Eng. 40 (1) (1999) 1.
[37] E. Ruckenstein, Y.H. Hu, Appl. Catal. A 183 (1) (1999) 85.
[38] R.A. Flinn, P.K. Trojan, Engineering Materials and Their Applications, Houghton Mifflin Company, Boston, 1990.
[39] Y. Nagai, T. Yamamoto, T. Tanaka, S. Yoshida, T. Nonaka, T. Okamoto, A. Suda, M. Sugiura, Catal. Today 74 (3–4) (2002) 225.
[40] H.P. Klug, L.E. Alexander, X-ray Diffraction Procedures for Polycrystalline and Amorphous Materials, second ed. Wiley, New York, 1974.
[41] Q. Xu, A.K. Datye, K.C.C. Kharas, in: Proceedings of the Technical Program of the 17th North American Catalysis Society Meeting, Toronto, Ontario, Canada, June 2001.
[42] S.B. Wang, G.Q. Lu, Appl. Catal. B 19 (3–4) (1998) 267.
[43] H.S. Roh, K.W.W.S. Jun, J.S. Dong, S.E. Chang, Y. Park, Y.I. Joe, Mol. Catal. A 181 (1–2) (2002) 137.
[44] M.C.J. Bradford, The carbon dioxide reforming of methane over supported metal catalysts, Pennsylvania State University thesis, University Park, 1997.
[45] M. Boudart, G. Djega-Mariadassou, Kinetics of Heterogeneous Catalytic Reactions, Princeton University Press, Princeton, 1984.
[46] T. Horicuchi, T. Osaki, T. Sugiyama, K. Suzuki, T. Mori, J. Coll. Inter. Sci. 204 (1998) 217.
[47] J.R. Rostrup-Nielsen, in: J.R. Anderson, M. Boudart (Eds.), Catalysis—Science and Technology, Springer-Verlag, 1984, p. 1 (Chapter 5).
[48] J.H. Bitter, K. Seshan, J.A. Lercher, J. Catal. 171 (1) (1997) 279.
[49] J.H. Bitter, K. Seshan, J.A. Lercher, J. Catal. 183 (2) (1999) 336.

[50] J.H. Edwards, A.M. Maitra, Fuel Process. Technol. 42 (2–3) (1995) 269.
[51] J.R.H. Ross, A.N.J. van Keulen, M.E.S. Hegarty, K. Seshan, Catal. Today 30 (1–3) (1996) 193.
[52] S.-H. Lee, W. Cho, W.-S. Ju, B.-H. Cho, Y.-C. Lee, Y.-S. Baek, Catal. Today 87 (2003) 133.
[53] S.-H. Lee, W. Cho, W.-S. Ju, J.-S. Chang, S.-E. Park, Y.-S. Baek, in: Proceedings of the 7th International Conference on Carbon Dioxide Utilization, Seoul, Korea, October 12–16, 2003, p. 203.
[54] C. Song, W. Pan, S.T. Srimat, J. Zheng, Y. Li, Y.H. Wang, B.Q. Xu, Q.M. Zhu, Tri-reforming of methane over Ni catalysts for CO_2 conversion to syngas with desired H_2/CO ratios using flue gas of power plants without CO_2 separation, Stud. Surf. Sci. Catal. 153 (2004) 315.
[55] M. Halmann, A. Steinfeld, in: Proceedings of the 17th International Conference on Efficiency, Costs, Optimization, Simulation and Environmental Impacts of Energy and Process Systems, Guanajuato, México, July 7–9, 2004 (Paper no. 185).
[56] T. Inui, Catal. R. Soc. Chem. 16 (2002) 133.
[57] C. Song, in: Proceedings of the 2nd Topical Conference on Natural Gas Conversion and Utilization, Held in conjunction with AIChE 2002 Spring National Meeting, New Orleans, March 11–14, 2002, p. 402.